CHANNEL ESTIMATION REFINEMENT BY TRAINING SEQUENCE EXTENSION AND INTERLEAVER DESIGN

A THESIS SUBMITTED TO
THE GRADUATE SCHOOL OF NATURAL AND APPLIED SCIENCES
OF
MIDDLE EAST TECHNICAL UNIVERSITY

BY

SAMET GELİNCİK

IN PARTIAL FULFILLMENT OF THE REQUIREMENTS
FOR
THE DEGREE OF MASTER OF SCIENCE
IN
ELECTRICAL AND ELECTRONICS ENGINEERING

SEPTEMBER 2014

Approval of the thesis:

CHANNEL ESTIMATION REFINEMENT BY TRAINING SEQUENCE EXTENSION AND INTERLEAVER DESIGN

submitted by **SAMET GELİNCİK** in partial fulfillment of the requirements for the degree of **Master of Science in Electrical and Electronics Engineering Department, Middle East Technical University** by,

Prof. Dr. Canan Özgen
Dean, Graduate School of **Natural and Applied Sciences** ________________

Prof. Dr. Gönül Turhan Sayan
Head of Department, **Electrical and Electronics Engineering** ________________

Assoc. Prof. Dr. Ali Özgür Yılmaz
Supervisor, **Electrical and Electronics Eng. Dept.,METU** ________________

Examining Committee Members:

Prof. Dr.Yalçın Tanık
Electrical and Electronics Engineering Dept., METU ________________

Assoc. Prof. Dr. Ali Özgür Yılmaz
Electrical and Electronics Engineering Dept., METU ________________

Prof. Dr. Tolga Çiloğlu
Electrical and Electronics Engineering Dept., METU ________________

Prof. Dr. T. Engin Tuncer
Electrical and Electronics Engineering Dept., METU ________________

Prof. Dr. Tolga Mete Duman
Electrical and Electronics Engineering Dept., Bilkent University ________________

Date: 04.09.2014

I hereby declare that all information in this document has been obtained and presented in accordance with academic rules and ethical conduct. I also declare that, as required by these rules and conduct, I have fully cited and referenced all material and results that are not original to this work.

Name, Last Name: SAMET GELİNCİK

Signature :

ABSTRACT

CHANNEL ESTIMATION REFINEMENT BY TRAINING SEQUENCE
EXTENSION AND INTERLEAVER DESIGN

Gelincik, Samet
M.S., Department of Electrical and Electronics Engineering
Supervisor : Assoc. Prof. Dr. Ali Özgür Yılmaz

September 2014, 57 pages

Rapid variation of channel coefficients is one of the most challenging problems in wireless communication. To provide and keep communication in desired quality, channel coefficients should be estimated continuously. This can be made by using pilot symbols between data blocks which are known by the transmitter and receiver. The channel coefficients between pilot symbols can be estimated by interpolation but this method has a disadvantage in fast fading channels since the channel coefficient estimates have better quality around the pilot blocks than away from them. To solve this problem, we propose to extend the pilot block by making use of the soft information produced by channel decoder. We track the channel estimates in time by the LMS algorithm bidirectionally so that we can estimate coefficients more accurately by interpolation . We also introduce a new interleaver which divides the bits into subregions based on their proximity to pilot blocks and permutes them within their own region.

Keywords: Sum product algorithm, Soft input soft output equalization, channel estimation, least square estimation, least mean square algorithm, interleaver

ÖZ

DENEME DİZİSİ GENİŞLETİMİ VE KARIŞTIRICI TASARIMIYLA KANAL KESTİRİMİ İYİLEŞTİRMESİ

Gelincik, Samet
Yüksek Lisans, Elektrik ve Elektronik Mühendisliği Bölümü
Tez Yöneticisi : Doç. Dr. Ali Özgür Yılmaz

Eylül 2014, 57 sayfa

Kanal katsayılarının hızlı değişimi kablosuz haberleşmenin en önemli problemlerinden biridir. Kaliteli bir iletişimin sağlanması ve sürdürülebilmesi için kanal katsayılarının sürekli kestirilmelidir. Bu ise veri bloklarının arasında gönderilecek alıcı ve verici tarafından bilinen deneme sembolleri vasıtasıyla yapılabilir. Pilot sembolleri arasındaki kanal katsayıları aradeğerleme yöntemiyle bulunabilmesine rağmen bu yöntem hızlı değişen kanallarda deneme sembollerinin yakınlarında kanalı iyi takip etmesine rağmen özellikle kanalın ortasına doğru kanalı takip edememektedir. Biz bu çalışmada yukarıda belirttiğimiz aradeğerlemenin yetersiz kalma problemine çözüm olarak, deneme sembollerinin etrafındaki veri sembollerini kullanarak kanalı deneme sembollerinin etrafındaki belli noktalara kadar LMS yöntemiyle takip etmeyi ve bundan sonra aradeğerleme yapmayı önerdik. Ayrıca bu uyguladığımız yönteme uygun, zaman ekseninde bir çeşit çoklama sağlayan bir karıştırıcı tasarlayarak iletişim kalitesini arttırdık.

Anahtar Kelimeler: Toplam çarpım algoritması, yumuşak girdili yumuşak çıktılı kanal denkleştirme, kanal kestirimi, en az kareler kestirimi, en az karesel ortalama algoritması, karıştırıcı

To my family

ACKNOWLEDGMENTS

First, I would like to thank my supervisor, Ali Özgür Yılmaz, for his continuous support and mentorship which guide me in both academic and personal life. It is a great pleasure to work in new and exciting concepts in communications with such a successful and modest advisor for me.

I am indebted to my first friends in the room C-206 Selim Özgen, Enver Ekmekçi and Ahmet Elbir for helping me get used to academic environment. Special thanks to Tuğcan Aktaş and Pınar Şen for their invaluable friendship and motivating chat in my hard times. Also, thanks to our new group members Ali Bulut Üçüncü and Alptekin Yılmaz Yunuscan Gültekin for their pleasant talk. Very special thanks to my friends, Fatih Özçelik, Nurettin Sezer, Abdülkerim Çengeloğlu and especially Mustafa Ergül and Mehmet Akif Akkuş because of their help. Moreover, I thank all of my friends who are not mentioned here for all their contributions to my personality and my life.

Thanks to the research project supported by Aselsan A.Ş., I had a chance to work with Ali Özgür Yılmaz and to focus on the core subject of our study which is developed and presented here.

I thank my family for being so supportive and caring parents. It is priceless to know that they always stand behind me with their unconditional love. My brother and house mate Cemal has a very special place in my life. Alongside of our invaluable memories since our childhood, I am grateful for his relaxing and cheerful personality which has a healing effect on me in my hard times.

TABLE OF CONTENTS

LIST OF TABLES

TABLES

LIST OF FIGURES

FIGURES

LIST OF ABBREVIATIONS

APP	A Posteriori Probability
AR	Auto-regressive
AWGN	Additive White Gaussian Noise
PER	Packet-Error-Rate
BPSK	Binary Phase Shift Keying
BCJR	Bahl-Cocke-Jelinek-Raviv
FDE	Frequency Domain Equalization
GMP	Gaussian Message Passing
ISI	Inter-Symbol Interference
JG	Joint Gaussian
LMMSE	Linear Minimum Mean Square Error
LLR	Log-likelihood Ratio
MSE	Mean Square Error
pdf	Probability Density Function
PSD	Power Spectral Density
PSK	Phase Shift Keying
QAM	Quadrature Amplitude Modulation
rRC	Root-Raised-Cosine
SC-FDE	Single Carrier Frequency Domain Equalization
SISO	Soft in Soft Out
SNR	Signal-to-Noise Ratio
ZMCSCG	Zero Mean Circularly Symmetric Complex Gaussian

CHAPTER 1

INTRODUCTION

Signals transmitted through wireless channels are exposed to various adverse effects due to the nature of the wireless medium. One of these effects is multipath propagation which is the result of reflection, refraction or diffraction. Multipath propagation reproduces many copies of the transmitted signal where a receiver antenna observes multiple echoes in different delays and attenuations. When the multipath delay is greater than the symbol duration, interference across symbols (inter-symbol interference (ISI)) forms. Multipath propagation also causes fluctuation in received signal power which is called fading. Furthermore, changes of communication medium makes the channel time varying. To reconstruct the transmitted signal at the receiver side channel estimation and equalization must be carried out.

In many scenarios channel estimation is an integral part of the receiver design. In the literature, there are three different channel estimation techniques: blind, semi blind and training based. Blind channel estimation [28] method is based on estimating the channel using known statistics about the channel and input sequence, not through known symbols. However, it has some disadvantages such as convergence, latency, phase ambiguity etc. To overcome such problems, semi blind channel estimation methods [28] are suggested so that fast and robust estimation can be provided by means of using known symbols and known statistics about data symbols [11]. The semi blind estimation can also be used efficiently in estimating fast fading channels and has superiority over training based and blind channel estimation separately [11]. Training-based channel estimation is executed in various ways through transmission of symbols known both to transmitter and receiver. Some of the techniques used with training based estimation are Least Squares [31], correlation estimation [5], ML estimation [30]. As an example, training based channel estimation is used in Global System for Mobile Communication (GSM) [15] and EDGE [16].

Training based channel estimation is used effectively in case of slow time variation of the channel through pilot sequences transmitted periodically. In this case, the channel is estimated at pilot regions and then interpolated for the data regions by various interpolators such as linear [6], Wiener filtering [7]. This approach is used in IS-136 [3]. However, when the time variation rate of the channel increases, interpolation aided training based channel estimation is not effective especially because of throughput inefficiency since it requires transmitting pilot sequences more frequently. To enable channel estimation in relatively fast fading channels, there are several methods in the literature for iterative receivers. In [27] and [24],a data aided channel estimation method is proposed in which the channel is iteratively estimated through soft information of the channel decoder by using some techniques such as LMS, RLS, Kalman filtering. As an alternative to those methods, we propose another data directed training based channel estimation method. The method iteratively extends pilot sequence to portions of data which is estimated through the soft information produced by decoder. With this "extended training sequence", the channel can be tracked bidirectionally inside the extended training sequence regions. Then, interpolation provides better quality channel estimation along a whole packet.

In Chapter 2, the background information needed through the thesis can be found. In Chapter 3, both the sum product (SP) algorithm which is an implementation of soft input soft output (SISO) equalizer and the utilized SISO equalizer structure is described. In Chapter 4, channel estimation with the least squares (LS) algorithm, the pilot extension idea, tracking of the channel with the LMS algorithm, interleaver design are explained and related results are provided. Conclusions follow in chapter 5.

The employed notations are organized as follows. Lower case letters (e.g., x) represents scalars, bold letters (e.g., $\mathbf{x}$) denote vectors, bolded upper case letters (e.g., $\mathbf{X}$) denote matrices. For a given vector random variable $\mathbf{x}$, $\mathbf{R_x}$ denote its autocorrelation matrix. The indicators $()^H$, $()^*$, and $E\{\}$ denote Hermitian transpose, conjugate transpose and expectation operations respectively. The matrix $\mathbf{I}$ represents the identity matrix of proper size.

CHAPTER 2

BACKGROUND INFORMATION

2.1 Wireless Channel Characterization

2.1.1 Some Wireless Channel Features

Wireless transmission medium has many features different from those of fixed or wired channels and these features are the consequence of mobility and specific nature of the surrounding medium.

Multipath propagation is a very important phenomenon that has role on many problems which arise in wireless communication. During a wireless transmission, a transmitter and receiver may have a direct path between each other and it is called the line of sight path (LOS). However, the signal reaches the receiver through many different paths and this phenomenon is called multipath propagation resulting from many interacting objects surrounding the transmitter and receiver like houses, walls, doors or windows which the signal reflects and/or diffracts through them. These signals have various amplitude, phase and delay.

The deviation of a multipath signal experienced in relative phase of a frequency component or in amplitude is defined as fading and results in attenuation of the signal. The multipath components of a signal causes interference and this interference can be constructive or destructive depending on the phase of the arriving multipath components. Instantaneous deviation of the signal level is defined as small scale fading. Large- scale fading occurs if there is an obstacle in the propagation path so that one or many multipath components are attenuated greatly with the result of preventing the communication. The small and large scale fading are combined at the receiver and in practice, it results in changing the channel coefficients with time and sometimes signal power undergo noise level with the consequence of symbol error in an uncoded structure.

The maximum delay between multipath components of a symbol is defined as delay spread, T_m. Multipath signal components coming from different path lengths may cause interference at the receiver if a multipath component of a signal arrives the antenna at the same time with any subsequent signal. This situation arises if one of the delays between multipath components of a transmitted symbol is greater than a symbol duration. This phenomenon is called inter-symbol interference (ISI).

Movements of the transmitter and receiver or changes in the surrounding medium leads to variation of the multipath components' properties. This dynamic behaviour of the channel impulse response is usually characterized by Doppler spread of the channel which roughly describes the rate of change for the channel impulse response components. Assuming wide sense stationary channel impulse response, the variation in time is reflected in power spectral density (PSD). In our simulations, we will consider a Gaussian shaped PSD where the twice the standard deviation σ of the PSD will be referred to as fading bandwidth (FBW). FBW is also a measure for channel coherence time T_c. The coherence time is qualitatively defined as the range of values over which the autocorrelation of channel taps in time is nonzero. The relationship between the channel coherence time and FBW is

$$T_c \approx \frac{1}{FBW}. \tag{2.1}$$

2.1.2 Channel Model

In this thesis, we consider a channel model characterized as a discrete time baseband equivalent channel with the assumption that required conditions such as proper sampling and filtering are in effect [26]. The discrete time model for a time varying channel is

$$\mathbf{h}_n = [h_{n,0}, h_{n,1}, ..., h_{n,L-1}] \tag{2.2}$$

where n indicates the sampling time $nT + \tau_0$, T and τ_0 are symbol duration and an arbitrary time offset. The index k in $h_{n,k}$ indicates the response of channel with delay kT at the time instant $nT + \tau_0$ and L indicates the total channel length.

In the time invariant case, the time index n is dropped since the channel is constant the whole observation time so that

$$\mathbf{h} = [h_0, h_1, ..., h_{L-1}]\,. \tag{2.3}$$

2.2 The HF Communication

The High Frequency (HF) band is defined as the electromagnetic spectrum between 3 MHz and 30 MHz, which corresponds to wavelengths between 10 m and 100 m. The radio communication which is performed in this frequency band is called HF communication. The detailed information about HF communication can be found in [18] and [17].

HF communication is very often used for military purposes. Military communication standards are being developed by NATO (North Athlantic Treaty Organization), and by US DoD (United States Department of Defence). The STANAG (Standardization Agreement) series is published by NATO , the MIL-STD (Military Standard) series is published by US DoD. With the introduction of some new standards such as STANAG 4539, Military Standard 188110-C, the performance is improved in terms of availability and data rates.

2.2.1 Propagation Mechanism

There are two major propagation mechanisms for electromagnetic waves in the HF band. One of them is ground wave in which the waves propagate along the surface of the earth. The other one is sky wave in which the waves are reflected back to the earth from the ionosphere. Transmission frequency and conductivity of the surface of the earth determines the propagation range of the ground wave.

Sky wave is used for communication distances of at least 50 km by using one or more reflection between earth and ionosphere layers. When the electromagnetic waves from the sun is absorbed by the athmosphere, molecules are ionized. The density profile of different types of molecules, the solar zenith angle and the strength of the ionizing electromagnetic waves determine the ionization which is concentrated in layers or regions. Since ionization depends on the solar zenith angle, it is denser during day than during night, and denser in summer than in winter. The solar activity and the 11-year sunspot cycle change the ionization density.

The lowest altitude, between 60-90 km, of the ionosphere corresponds to layer D and it has lower electron density respect to layer D and F so that does not reflect the radio waves. However, it absorbs the energy of waves. The middle layer is layer E and the altitude is between 90 and 120 km. The layer F is highest altitude and it includes the altitude between 200 and more than 500 km. The E and F regions electron density is enough to refract electromagnetic waves in HF range so these two regions act as a reflector for HF communication.

The received noise in HF frequencies consists of man made noise, galactic noise and athmospheric noise (static discharge). This noise is investigated in [13] and it may has a bursty nature. However, it can be modelled as band-limited additive White Gaussian noise with a simplifying assumption. More details can be found in [20].

2.2.2 HF Channel

The transmitter and receiver are not moving (or moving slowly relative to the wavelength) in ionospheric HF communication system. However, the electromagnetic waves are being reflected from large number of randomly moving ions. This means that the Doppler shift can be modelled by Gaussian distribution [22]. This model is verified experimentally by Watterson, Juroshek and Bensema in [29]. The model is referred as Watterson model in literature.

The Watterson channel is a two tap channel with the delay spread values quite large in the vicinity of a few milliseconds. The taps are independent and have equal power with the Gaussian PSD.

Assuming the mean of Doppler shift is zero, the Gaussian Doppler spectrum can be written as

$$S_h(\upsilon) = \frac{1}{\sqrt{2\pi\sigma_\upsilon^2}} \exp\left(-\frac{\upsilon^2}{2\sigma^2}\right) \tag{2.4}$$

where σ_υ^2 is the variance of the Doppler shift. For a fading channel which has Gaussian power spectral density, we define the Doppler spread or fading bandwith (FBW) as twice of the standard deviation of the Doppler shift

$$FBW = 2\sigma_\upsilon. \tag{2.5}$$

2.3 Channel Estimation Techniques

In the thesis, a data directed training based channel estimation technique will be used. Hence, the channel estimation method is based on using not only the known symbols and their corresponding observations, but also on observations of unknown data. It is imperative that training based channel estimation is basis of data directed channel estimation. Training based channel estimation is applied for time-invariant channels and in case of very short pilot sequence duration so that the channel varies slowly. Assuming a training sequence $\mathbf{x} = [x_0, x_1, ..., x_N]$, the corresponding output $\mathbf{y} = [y_0, y_1, ..., y_{N+L-1}]$ and the channel $\mathbf{h} = [h_0, h_1, ..., h_{L-1}]$, our discrete time system model is given in matrix form for the time-invariant case as [2]

$$\mathbf{y} = \mathbf{X}\mathbf{h} + \mathbf{w} \tag{2.6}$$

where $\mathbf{X}$ is an $N + L - 1 \times L$ matrix whose rows are shifts of training sequence and $\mathbf{w} = [w_0, w_1, ..., w_{N+L-1}]$ is composed of circularly symmetric complex additive white Gaussian noise samples.

2.3.1 Least Squares Estimation

Least Squares (LS) channel estimation can be obtained from

$$\hat{\mathbf{h}}_{LS} = argmin_{\mathbf{h}} \left(\mathbf{y} - \mathbf{X}\mathbf{h}\right)^H \left(\mathbf{y} - \mathbf{X}\mathbf{h}\right). \tag{2.7}$$

The size of vector $\mathbf{y}$ is N which is the number of received signals affected by only the training symbols. The LS estimation of channel can be found by the equation [2]

$$\hat{\mathbf{h}}_{LS} = \left(\mathbf{X}^H\mathbf{X}\right)^{-1} \mathbf{X}^H\mathbf{y}. \tag{2.8}$$

2.3.2 Maximum Likelihood Estimation

With maximum likelihood (ML) channel estimation, the coefficients which maximizes the likelihood of the received signal is searched for:

$$\hat{\mathbf{h}}_{ML} = argmax_{\mathbf{h}} p\left(\mathbf{y} \mid \mathbf{h}\right). \tag{2.9}$$

For complex Gaussian noise, the solution can be obtained by maximizing the equation given in [2]

$$\hat{\mathbf{h}}_{ML} = argmax_{\mathbf{h}} \left(\mathbf{y} - \mathbf{X}\mathbf{h}\right)^H \mathbf{R}_w^{-1} \left(\mathbf{y} - \mathbf{X}\mathbf{h}\right) \tag{2.10}$$

which is related to the logarithm of the ML function where R_w is the covariance matrix of noise. In that case, the ML estimate of the channel is given in [2] as

$$\hat{\mathbf{h}}_{ML} = \left(\mathbf{X}^H\mathbf{R}_w^{-1}\mathbf{X}\right)^{-1} \left(\mathbf{X}^H\mathbf{R}_w^{-1}\right)\mathbf{y}. \tag{2.11}$$

However, in case of zero mean circularly symmetric white Gaussian noise, $R_w = N_0\mathbf{I}$ and the ML estimate can be calculated with

$$\hat{\mathbf{h}}_{ML} = \left(\mathbf{X}^H\mathbf{X}\right)^{-1}\left(\mathbf{X}^H\right)\mathbf{y}. \tag{2.12}$$

It is seen from (2.12) and (2.8) that two estimation techniques is matched if the noise is zero mean circularly symmetric white Gaussian noise.

2.4 Equalizer

From section 2.1.1, it is known that ISI occurs if delay spread T_m is greater than symbol duration T. ISI prevents correct symbol and bit decoding unless special measures are not taken even in high signal-to-noise ratios (SNR). In a broad manner, any signal processing method which alleviates ISI is called equalization. Equalization can be implemented through one of filtering, sequence estimation or iterative techniques.

There are two main types of equalizers in the literature: linear and non-linear. Some linear equalizer types can suffer from noise enhancement [14] which results in SNR degradation even though ISI is completely eliminated. Non linear equalization methods have less noise enhancement but it has larger implementation complexity. Equalization techniques requires channel impulse response to mitigate the ISI. In time varying cases, the equalizer tracks the change in channel with the aid of training symbols through some updating methods, i.e. LMS, RLS, Kalman filtering etc., which are categorized as adaptive equalization.

Two of the popular linear equalizers are zero forcing (ZF) and minimum mean square (MMSE) equalizers. ZF equalizers eliminate all ISI introduced by the channel but has trouble with noise enhancements. MMSE equalizer works in the sense which minimizes mean square error between the transmitted symbols and their corresponding equalizer outputs so that its noise enhancement problem is less than ZF equalizer but it does not eliminate all ISI. In short, the MMSE equalizers balance ISI mitigation and noise enhancement.

Nonlinear equalizer examples are decision feedback equalizer (DFE) and maximum likelihood sequence estimaton (MLSE). DFE uses previously estimated symbols to alleviate ISI through a feedback filter and does not suffer from noise enhancement. Also

DFE generally has superiority over linear equalizers in deep fading cases [14] despite its error propagation problems. MLSE has no problem with noise enhancement since it is not implemented with any filter. MLSE algorithm provides the sequence which maximizes likelihood of the received signal. It is the optimal equalization for and used as lower bound in the sense of minimizing sequence error. However, its implementation complexity prevents widespread use.

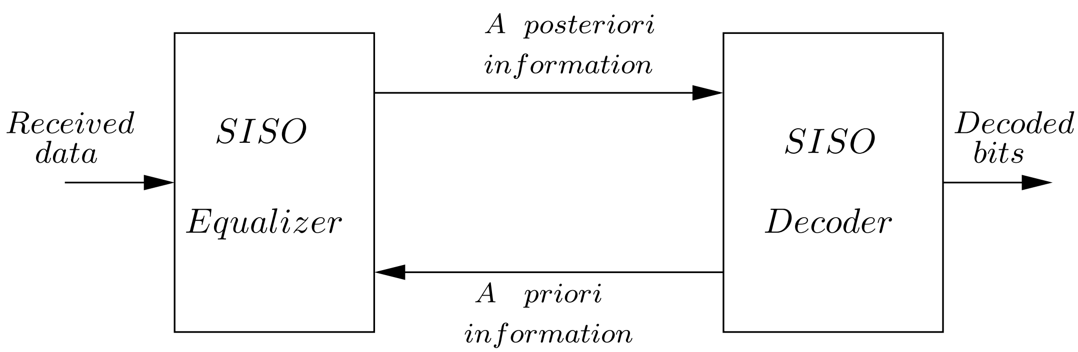

Figure 2.1: Turbo Equalizer

In iterative (turbo) equalization processes such as in Fig. 2.1, probability information, called soft information, related to symbols or bits are usually exchanged between equalizer and decoder to determine the transmitted symbols. Therefore, the equalizer which operates in turbo equalization is usually in the form of a soft input soft output (SISO) equalizer and provides a posteriori probabilities (APP's) of transmitted bits to the channel decoder and the decoder provides the a priori informations of symbol to the equalizer.

2.4.1 Interleaver

In wireless communication, fading is an essential problem leading to received power being lower than noise level in severe conditions so that errors occur in transmission of information. Moreover, in some cases such a severe fading continues a long period of time leading to many consecutive errors, called burst errors. Although error correcting codes (ECC) mitigate the errors induced by the channel, many widely used ECC codes, e.g., convolutional codes, operates under the assumption of independent bit/symbol errors. Interleaving is an effective solution to roughly create such a scenario with burst errors. Interleaver is defined as a single input single output device which takes the symbol sequence in a fixed alphabet and produces the same sequence in a different order. The classical usage of interleaver is to separate the consecutive bits to minimize the burst error probability by way of transforming the channel as if errors occur in regions apart from each other. A similar scenario is needed in turbo decoding and equalization. Hence interleaving is usually present in turbo decoding and equalization systems [26].

We will utilize block interleavers in this work. In a block interleaver data is written in row-wise in a matrix form and read in column-wise from that matrix. A pseudo random block interleaver is a sort of block interleaver in which data is written a sequential manner and read out in a pseudo random order.

2.5 System Model

2.5.1 General Model

Consider the system shown in Fig. 2.2. A block of data bits $b_l \in \{1, 0\}$ are convolutionally encoded with a rate R_c to form coded bits $c_{p'} \in \{1, 0\}$, then the coded bits are interleaved to c_p by employing a permutation function $\Pi(.)$. Throughout this work, gray mapping is used for modulation where Q consecutive coded bits $c_{(n-1)Q+i}$, $i \in \{1, 2, .., Q\}$ are combined to form a symbol z_n in $\mathbf{S} = \{s_1, s_2, ..., s_{2^Q}\}$. The constellations are phase shift keying (PSK) and quadrature amplitude modulation (QAM). In addition to data symbols, training and synchronization symbols which are known by receiver are added to data sequence to form transmitted symbols $x_n, n \in \{1, 2, ..., N\}$. Then x_n are modulated with a carrier at a symbol rate f_s symbols per second. Symbol spaced discrete time model for sending the symbols x_n through the intersymbol interference (ISI) channel produces the received symbols

$$y_n = \mathbf{h}^T \mathbf{x}_n + w_n \tag{2.13}$$

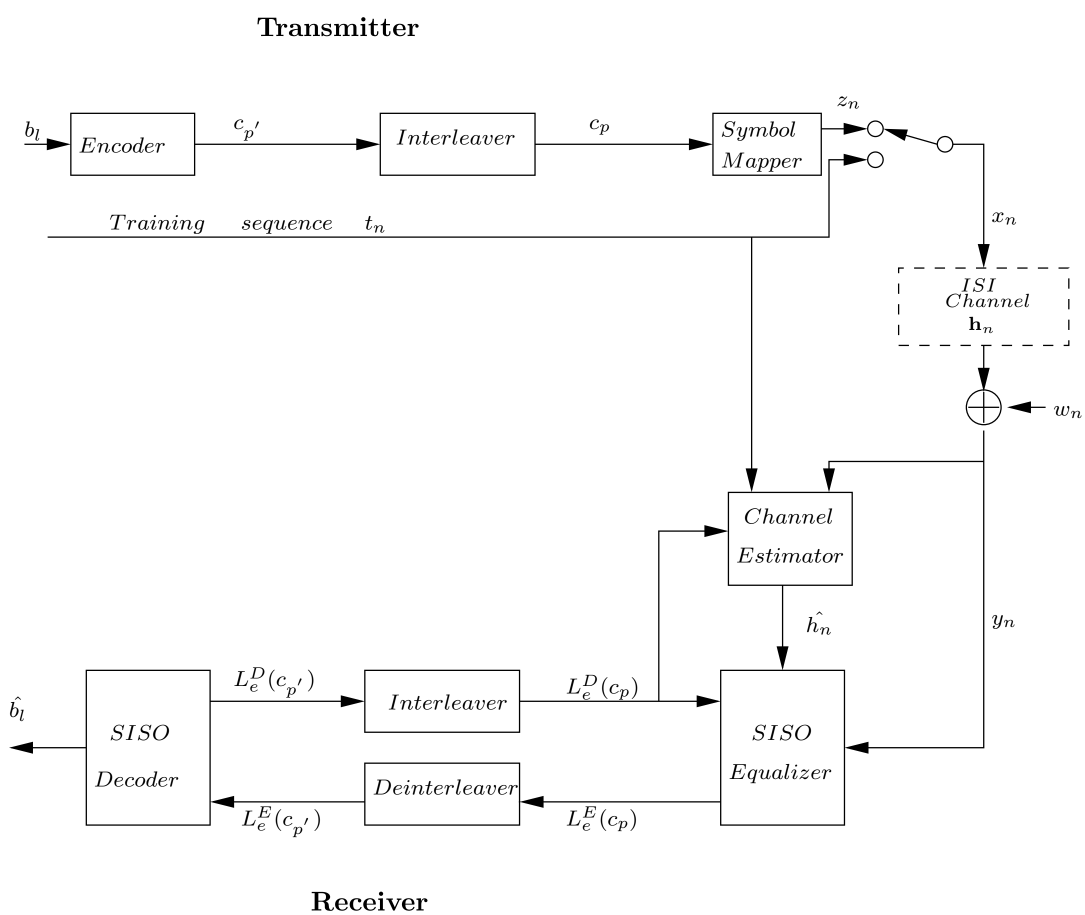

Figure 2.2: Reference system model using adaptive turbo equalization in the receiver

where $\mathbf{h}_n = [h_{n,0}, ..., h_{n,L-1}]$ is the time varying channel impulse response (CIR) at time n with length L and $\mathbf{x}_n = [x_n, x_{n-1}, ..., x_{n-L+1}]$. The scalar w_n denotes independent and identically distributed zero mean circularly symmetric complex Gaussian random variables, where real and imaginary parts are independent and have the same variance $\sigma^2 = N_0/2$. It is more compact to write the transmission model in matrix form. Thereby, in case of the transmitted symbol sequence $\mathbf{x} = [x_1, x_2, ..., x_N]$, the received signal can be written

$$\mathbf{y} = \mathbf{H}\mathbf{x} + \mathbf{w} \tag{2.14}$$

with

$$\mathbf{H} = \begin{bmatrix} h_{0,0} & & 0 & \ldots & \ldots & 0 \\ \vdots & \ddots & & 0 & \ldots & 0 \\ h_{L-1,L-1} & & \ldots & h_{L-1,0} & & \vdots \\ 0 & \ddots & & \ddots & & \\ \vdots & & \ddots & & \ddots & 0 \\ & & & h_{N,L-1} & \ldots & h_{N,0} \\ & & & & \ddots & \vdots \\ 0 & & \ldots & & 0 & h_{N+L-1,L-1} \end{bmatrix}. \tag{2.15}$$

where $\mathbf{y} = [y_1, y_2, ..., y_{N+L-1}]$ and $\mathbf{w} = [w_1, w_2, ..., w_{N+L-1}]$.

At the receiver side, the SISO equalizer produces extrinsic information LLRs $L_e^E(c_p)$ as input to the SISO decoder after deinterleaving. The decoder yields the estimates of information bits $\hat{b}_l$ and extrinsic LLRs $L_e^D(c_{p'})$ which are interleaved to $L_e^D(c_p)$ as input to the equalizer. Iterative channel estimation refinement is possible by using an extended training sequence which are estimated by LLR information $L_e^D(c_p)$ produced by the SISO decoder.

2.5.2 Specific Model

Information bits are convolutionally encoded with a rate $R_c = 1/2$ and constraint length 7. The coded bits are interleaved by a block interleaver with respect to the permutation function given in Military Standard 188-110C (ML-188110C). The transmitted signal frame structure is adopted from (ML-188110C) and shown in Fig. 2.3. A transmitted signal frame consists of a synchronization preamble followed by 16 data blocks, 544 symbols each of which has pilot block at both sides. Thereby a frame includes 17 pilot blocks totally. Each of pilot block has 68 symbols. The pilots are modulated with 8 PSK and the data sequence is modulated with BPSK or 4-QAM. The transmitted sequence is sent at a a rate of 4800 symbols per second and the pulse shaping function is raised cosine with a roll-off factor of 0.35. The transmitted channel is Watterson channel which has two independent taps with rayleigh fading [10] with the Gaussian power spectral density (PSD). The channel length is 10 and the two taps have equal power.

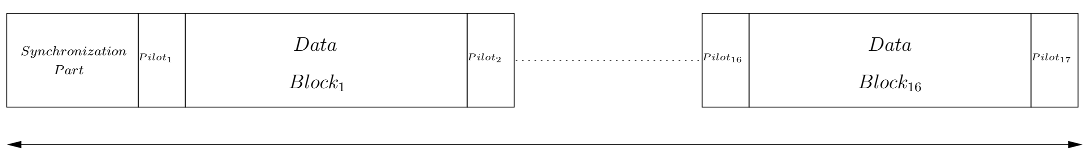

Figure 2.3: Transmitted signal frame

In the receiver part, we assume exact synchronization between transmitter and receiver because synchronization preamble long enough to provide correct synchronization between transmitter and receiver. Therefore, the synchronization part is not considered in simulations. The equalizer is a SISO equalizer which is implemented through the sum product (SP) algorithm [21]. The channel is initially estimated with the least-squares (LS) algorithm in pilot regions, the data regions are interpolated with spline interpolation method and channel tracking is performed by the least-mean-square (LMS) algorithm.

CHAPTER 3

THE SUM PRODUCT ALGORITHM AND SOFT-INPUT SOFT-OUTPUT (SISO) EQUALIZER

3.1 Introduction

In our work, our interest is HF communication. It is known that HF channel is modelled as a time varying inter-symbol interference (ISI) channel [23] so that an equalizer is utilized in the receiver side to alleviate ISI. Our receiver (in Section 2.5) performs turbo equalization which exchanges soft information between equalizer and decoder. Therefore our equalizer should be a soft in soft out (SISO) component, which is also called SISO equalizer. The early SISO equalizers were based on trellis based algorithms [4] and [12]. However, the number of trellis states becomes excessive size when the channel impulse response (CIR) is very large and the signal constellation is large [25]. This makes trellis based SISO equalization impractical for HF communication since the corresponding channel lengths are long generally. Despite some performance degradation suboptimal SISO equalizers based on soft ISI cancellation and linear filtering methods are utilized to overcome practical difficulties.

The SISO equalization can provide marginal a posteriori probabilities (MAP) of the transmitted symbols with soft ISI cancellation. In so doing, one has to marginalize the joint probability density function of transmitted vector given the received vector in order to compute the MAP of transmitted symbols. SISO equalization implemented on a suitable factor graph (FG) is an attractive option in the sense of complexity and practicality.

In this chapter, firstly we provide some fundamental information about FGs and the Sum Product (SP) algorithm and later present graph based SISO equalizer [8].

3.2 Sum Product Algorithm

The SP algorithm operates on suitable factor graphs for the marginalization with respect to some local function over variables of a global function. Considering a set of variables $x_1, x_2, ...x_n$, and subsets $\chi_{\mathbf{i}}$ of this set of variables, a global function is written first for a particular problem in its factorized form:

$$g\left(x_1, x_2, ...x_n\right) = \prod_i g_i\left(\chi_{\mathbf{i}}\right). \tag{3.1}$$

Based on this factorized representation, one may draw a FG as in Fig. 3.1 where the related variables and functions are linked. It has been known [21] that marginalization $g\left(x_i\right) = \sum_{\sim x_i} g\left(x_1, x_2, ..., x_n\right)$ can be often performed effectively over the set of variables excluding x_i which is denoted by $\sim x_i$.

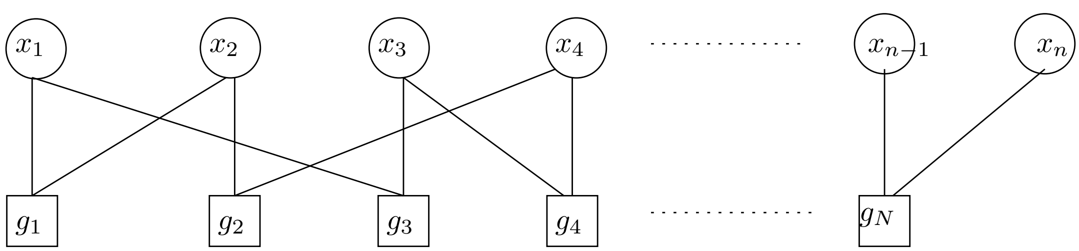

Figure 3.1: A factor graph for
$g\left(x_1, x_2, ...x_n\right) = g_1\left(x_1, x_2\right) g_2\left(x_2, x_4\right) g_3\left(x_1, x_3\right)$
$g_4\left(x_3, x_4\right) ....g_N\left(x_{n-1}, x_n\right)$

In the factor graph of Fig. 3.1, g_i's and x_i's are defined as function nodes and variable nodes respectively and the message passings are executed between these nodes for marginalization. The messages are computed based on the formulations below:

• the message from a variable node to a function node:

$$\mu_{x_i \to g_j}(x_i) = \prod_{g_k \in n(x_i) \setminus \{g_j\}} \mu_{g_k \to x_i}(x_i), \tag{3.2}$$

• the message from a function node to a variable node:

$$\mu_{g_j \to x_i}(x_i) = \sum_{\sim \{x_i\}} \left(g_j(\chi_{\mathbf{j}}) \prod_{x_k \in n(g_j) \setminus \{x_i\}} \mu_{x_k \to g_j}(x_k) \right). \tag{3.3}$$

In the formulations above, $n(g_j)$ is the argument set of the function g_j and $n(x_i)$ is the set of functions of which x_i is element. Also, "$\sim$" indicates the summing operation over the variables except the corresponding variable. This operation is defined as the summary operation. By this way, we send marginal function of corresponding variable.

At every iteration of the SP algorithm the marginal function of variables are updated where an iteration is defined as the message passing from all variables to all corresponding nodes and then message passing from all function nodes to all their corresponding variable nodes. In that case, the updated marginalized functions calculated as the product of all incoming messages to variable nodes are

$$f(x_i) = \prod_{g_k \in n(x_i)} \mu_{g_k \to x_i}(x_i). \tag{3.4}$$

3.3 A Specific Example

A more specific example of sum-product iteration over the function

$$f(\mathbf{x}) = f_1(x_1, x_2) f_2(x_2, x_3, x_4) f_3(x_3, x_5) f_4(x_2, x_4) f_5(x_4, x_5) \tag{3.5}$$

is described in steps below. The corresponding factor graph is depicted in Fig.(3.2).

• Step 1:

$\mu_{x_1 \to f_1}(x_1) = 1$

$\mu_{x_2 \to f_2}(x_2) = \mu_{f_4 \to x_2}(x_2)$

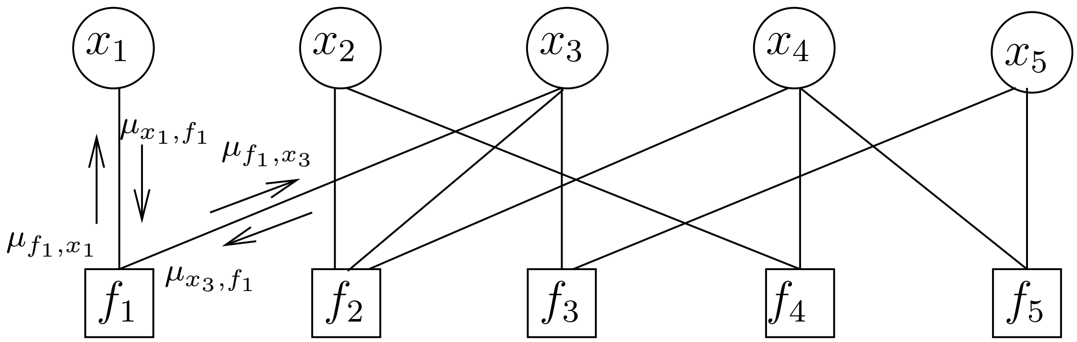

Figure 3.2: A factor graph for
$f\left(x_1,x_2,x_3,x_4,x_5\right)=f_1\left(x_1,x_3\right)f_2\left(x_2,x_3,x_4\right)f_3\left(x_3,x_5\right)f_4\left(x_2,x_4\right)f_5\left(x_4,x_5\right)$

$\mu_{x_2\to f_4}\left(x_2\right)=\mu_{f_2\to x_2}\left(x_2\right)$

$\mu_{x_3\to f_1}\left(x_3\right)=\mu_{f_2\to x_3}\left(x_3\right)\mu_{f_3\to x_3}\left(x_3\right)$

$\mu_{x_3\to f_2}\left(x_3\right)=\mu_{f_1\to x_3}\left(x_3\right)\mu_{f_3\to x_3}\left(x_3\right)$

$\mu_{x_3\to f_3}\left(x_3\right)=\mu_{f_1\to x_3}\left(x_3\right)\mu_{f_2\to x_3}\left(x_3\right)$

$\mu_{x_4\to f_2}\left(x_4\right)=\mu_{f_4\to x_4}\left(x_4\right)\mu_{f_5\to x_4}\left(x_4\right)$

$\mu_{x_4\to f_4}\left(x_4\right)=\mu_{f_2\to x_4}\left(x_4\right)\mu_{f_5\to x_4}\left(x_4\right)$

$\mu_{x_4\to f_5}\left(x_4\right)=\mu_{f_2\to x_4}\left(x_4\right)\mu_{f_4\to x_4}\left(x_4\right)$

$\mu_{x_5\to f_3}\left(x_5\right)=\mu_{f_5\to x_5}\left(x_5\right)$

$\mu_{x_5\to f_5}\left(x_5\right)=\mu_{f_3\to x_5}\left(x_5\right)$

- Step 2:

$\mu_{f_1\to x_1}\left(x_1\right)=\sum_{\sim\{x_1\}}f_1\left(x_1,x_3\right)\mu_{x_3\to f_1}\left(x_3\right)$

$\mu_{f_1\to x_3}\left(x_3\right)=\sum_{\sim\{x_3\}}f_1\left(x_1,x_3\right)\mu_{x_1\to f_1}\left(x_1\right)$

$\mu_{f_2\to x_2}\left(x_2\right)=\sum_{\sim\{x_2\}}f_2\left(x_2,x_3,x_4\right)\mu_{x_3\to f_2}\left(x_3\right)\mu_{x_4\to f_2}\left(x_4\right)$

$\mu_{f_2\to x_3}\left(x_3,x_4\right)=\sum_{\sim\{x_3\}}f_2\left(x_2,x_3\right)\mu_{x_2\to f_2}\left(x_2\right)\mu_{x_4\to f_2}\left(x_4\right)$

$\mu_{f_2\to x_4}\left(x_4\right)=\sum_{\sim\{x_4\}}f_2\left(x_2,x_3x_4\right)\mu_{x_2\to f_2}\left(x_2\right)\mu_{x_3\to f_2}\left(x_3\right)$

$\mu_{f_3 \to x_3}(x_3) = \sum_{\sim\{x_3\}} f_3(x_3, x_5)\, \mu_{x_5 \to f_3}(x_5)$

$\mu_{f_3 \to x_5}(x_5) = \sum_{\sim\{x_5\}} f_3(x_3, x_5)\, \mu_{x_3 \to f_3}(x_3)$

$\mu_{f_4 \to x_2}(x_2) = \sum_{\sim\{x_2\}} f_4(x_2, x_4)\, \mu_{x_4 \to f_4}(x_4)$

$\mu_{f_4 \to x_4}(x_4) = \sum_{\sim\{x_4\}} f_4(x_2, x_4)\, \mu_{x_2 \to f_4}(x_2)$

$\mu_{f_5 \to x_4}(x_4) = \sum_{\sim\{x_4\}} f_5(x_4, x_5)\, \mu_{x_5 \to f_5}(x_5)$

$\mu_{f_5 \to x_5}(x_5) = \sum_{\sim\{x_5\}} f_5(x_4, x_5)\, \mu_{x_4 \to f_5}(x_4)$

Note that, since there is no message to variable x_1, the message from x_1 to function node f_1 is always 1. One iteration consists of these two steps. At the end of the iteration, if one wants to calculate marginal function of the variables

$f(x_1) = \mu_{f_1 \to x_1}(x_1)$

$f(x_2) = \mu_{f_2 \to x_2}(x_1)\, \mu_{f_4 \to x_2}(x_2)$

$f(x_3) = \mu_{f_1 \to x_3}(x_3)\, \mu_{f_2 \to x_3}(x_3)\, \mu_{f_3 \to x_3}(x_3)$

$f(x_4) = \mu_{f_2 \to x_4}(x_4)\, \mu_{f_4 \to x_4}(x_4)\, \mu_{f_5 \to x_4}(x_4)$

$f(x_5) = \mu_{f_3 \to x_5}(x_5)\, \mu_{f_5 \to x_5}(x_5)\,.$

In case of first iteration, all messages from a variable to a function node is unit message, because we assume incoming messages to a variable node was unit message [21]. After first iteration, all messages from variable nodes are executed as in step 1.

3.4 Soft-Input Soft-Output (SISO) Equalizer

Our one dimensional system model is based on linear modulations over linear channels affected by circularly symmetric complex white Gaussian noise. As a very general form, the relationship between the transmitted sequence $\mathbf{x} = [x_1, x_2, ..., x_N]^T$ and the received sequence $\mathbf{y} = [y_1, y_2, ..., y_{N+L-1}]^T$ can be written as in [26]

$$\mathbf{y} = \mathbf{H}\mathbf{x} + \mathbf{w} \tag{3.6}$$

with

$$
\mathbf{H} = \begin{bmatrix}
h_0 & & 0 & \dots & \dots & 0 \\
\vdots & & h_0 & 0 & \dots & 0 \\
h_{L-1} & & \dots & h_0 & & \vdots \\
0 & \ddots & & \ddots & & \\
\vdots & & \ddots & & \ddots & 0 \\
 & & & h_{L-1} & \dots & h_0 \\
 & & & & \ddots & \vdots \\
0 & & \dots & & 0 & h_{L-1}
\end{bmatrix}. \tag{3.7}
$$

where $\mathbf{w} = [w_1, w_2, ..., w_{N+L-1}]^T$ are independent and identically distributed zero-mean circularly symmetric complex Gaussian random variables, where real and imaginary parts are independent and have the same variance $\sigma^2 = N_0/2$. The channel convolutional matrix $\mathbf{H}$ has $K = N + L - 1$ rows and N columns where L is channel length.

In the equalization process, we want to compute MAP for symbols coming from finite modulation given the observation $\mathbf{y}$. To obtain MAP of the symbols individually, we factor the pdf of (3.6) suitably according to [8].

3.4.1 Maximum A Posteriori (MAP) Detection of Symbols

The MAP detection of symbols requires calculating a posteriori probabilities (APP's) of $p(x_n \mid \mathbf{y})$ for all n and x_n given the observation $\mathbf{y}$. This task can be accomplished based on $p(\mathbf{x} \mid \mathbf{y})$ through $P(\mathbf{x})$, a priori probability of the sequence of $\mathbf{x}$, and $p(\mathbf{y} \mid \mathbf{x})$, the conditional pdf of $\mathbf{y}$ given $\mathbf{x}$.

Since we assume that there is no correlation between transmitted sequence symbols, the probability of the sequence is written as

$$P(\mathbf{x}) = \prod_{n=1}^{N} P_n(x_n). \tag{3.8}$$

The conditional pdf of $\mathbf{y}$ given the transmitted sequence $\mathbf{x}$ equals

$$p(\mathbf{y} \mid \mathbf{x}) = \left(2\pi\sigma^2\right)^{-K} \exp\left(-\frac{\| \mathbf{y} - \mathbf{H}\mathbf{x} \|^2}{2\sigma^2}\right). \tag{3.9}$$

Since the factor $(2\pi\sigma^2)^{-K}$ is independent of the transmitted sequence $\mathbf{x}$, (3.9) can be written with a proportionality factor, which indicates that two quantities are different from each other by a constant factor independent of $\mathbf{x}$ as given below

$$p(\mathbf{y} \mid \mathbf{x}) \propto \exp\left(-\frac{\| \mathbf{y} - \mathbf{H}\mathbf{x} \|^2}{2\sigma^2}\right). \tag{3.10}$$

If we define

$$\mathbf{m} = \mathbf{H}^H \mathbf{y} \tag{3.11}$$

$$\mathbf{S} = \mathbf{H}^H \mathbf{H} \tag{3.12}$$

the norm square factor of (3.10) can be manipulated as

$$\begin{aligned} \| \mathbf{y} - \mathbf{H}\mathbf{x} \|^2 &= \mathbf{y}^{\mathbf{H}}\mathbf{y} - 2\Re\left\{\mathbf{x}^H \mathbf{H}^H \mathbf{y}\right\} + \mathbf{x}^H \mathbf{H}^H \mathbf{H}\mathbf{x} \\ &= \| \mathbf{y} \|^2 - 2\Re\left\{\mathbf{x}^H \mathbf{m}\right\} + \mathbf{x}^H \mathbf{S}\mathbf{x}. \end{aligned} \tag{3.13}$$

In that case (3.10) can be written as

$$p(\mathbf{y} \mid \mathbf{x}) \propto \exp\left(-\frac{\| \mathbf{y} \|^2 - 2\Re\left\{\mathbf{x}^H \mathbf{m}\right\} + \mathbf{x}^H \mathbf{S}\mathbf{x}}{2\sigma^2}\right). \tag{3.14}$$

One may note that $\mathbf{m}$ is a sufficient statistic (matched filter output) for MAP detection [26] and the $\| \mathbf{y} \|^2$ term does not depend on $\mathbf{x}$ so that

$$p(\mathbf{y} \mid \mathbf{x}) \propto \exp\left(\frac{2\Re\left\{\mathbf{x}^H\mathbf{m}\right\} - \mathbf{x}^H\mathbf{S}\mathbf{x}}{2\sigma^2}\right). \tag{3.15}$$

3.4.2 Graph-Based Detection Algorithm

Factorization of a function can be performed in multiple ways. In [8], a specific factorization was proposed to reduce the complexity of the sum-product algorithm to scale linearly with the number of interfering signal terms.

Some manipulations should be made on the (3.15) to have a suitable factor graph for SISO detection with SP algorithm. The scalar forms of matrix operations in (3.15) are

$$\mathbf{x}^H\mathbf{m} = \sum_{n=1}^{N} m_n x_n^* \tag{3.16}$$

$$\mathbf{x}^H\mathbf{S}\mathbf{x} = \sum_{n=1}^{N} S_{n,n} \mid x_n \mid^2 + \sum_{n=1}^{N} \sum_{k=1,k\neq n}^{N} x_n^* S_{n,k} x_k$$

since $\mathbf{S^H} = \mathbf{S}$,

$$\mathbf{x}^H\mathbf{S}\mathbf{x} = \sum_{n=1}^{N} S_{n,n} \mid x_n \mid^2 + \sum_{n=1}^{N} \sum_{k<n} 2\Re\left\{x_n^* S_{n,k} x_k\right\}. \tag{3.17}$$

By using these scalar forms, we can write the (3.15) as

$$p(\mathbf{y} \mid \mathbf{x}) = \prod_{n=1}^{N} \left[\exp\left(\frac{1}{\sigma^2}\Re\left\{m_n x_n^* - \frac{S_{n,n}}{2} \mid x_n \mid^2\right\}\right) \prod_{k<n} \exp\left(-\frac{1}{\sigma^2}\Re\left\{S_{n,k} x_k x_n^*\right\}\right)\right]. \tag{3.18}$$

In that case the function nodes $T_n(x_n)$ and $R_{n,k(x_n,x_k)}$ are defined as

$$T(x_n) = \exp\left(\frac{1}{\sigma^2}\Re\left\{m_n x_n^* - \frac{S_{n,n}}{2} \mid x_n \mid^2\right\}\right), \tag{3.19}$$

$$R_{n,k}\left(x_n, x_k\right) = \exp\left[-\frac{1}{\sigma^2}\Re\left\{S_{n,k}x_k x_n^*\right\}\right]. \tag{3.20}$$

By using these definitions and a priori probabilities of the transmitted sequence, we can factorize the APP density function

$$p\left(\mathbf{x} \mid \mathbf{y}\right) \propto P\left(\mathbf{x}\right) p\left(\mathbf{y} \mid \mathbf{x}\right) \propto \prod_{n=1}^{N}\left[P_n\left(x_n\right) T_n\left(x_n\right) \prod_{k<n} R_{n,k}\left(x_n, x_k\right)\right] \tag{3.21}$$

for which the factor graph in Fig. (3.3) is drawn.

As seen in Fig. 3.3, the node $R_{n,k}$ appears in FG, if $S_{n,k} \neq 0$, that is, when there is interference between the correspondingly nodes. Also, from (3.18) and hence the definition of (3.21) the node $R_{n,k}$ should be denoted as $R_{max(n,k),min(n,k)}$.

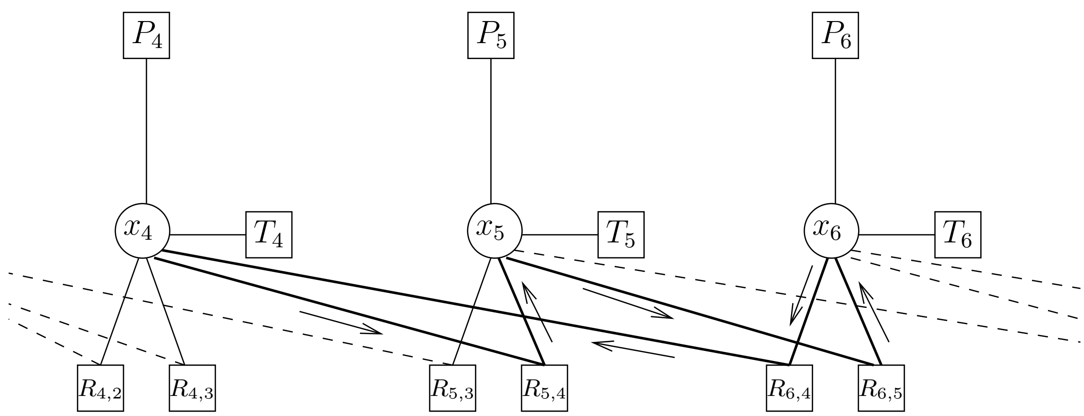

Figure 3.3: Some part of the factor graph respect to 3.21, when the interference exist between x_n and x_k if $\mid k-n \mid \in$ 1,2

There are some points to discuss to this end. The graph includes cycles, one of them is seen in Fig.3.3 as bold lines and the length of cycle is 6 because the cycle come back to the same variable in 6 steps as seen from arrows. The cycles indicates that the graph can not eliminate the effect of intersymbol-interference (ISI) due to the factorization. So, although the factorizaiton is exact, because there is no approximation in the derivation, the marginalization of (3.21) is not exact due to cycle in FG [21]. But in the case of cycle length is at least 6, the SP algorithm gives good results for the marginalization of APP's [21].

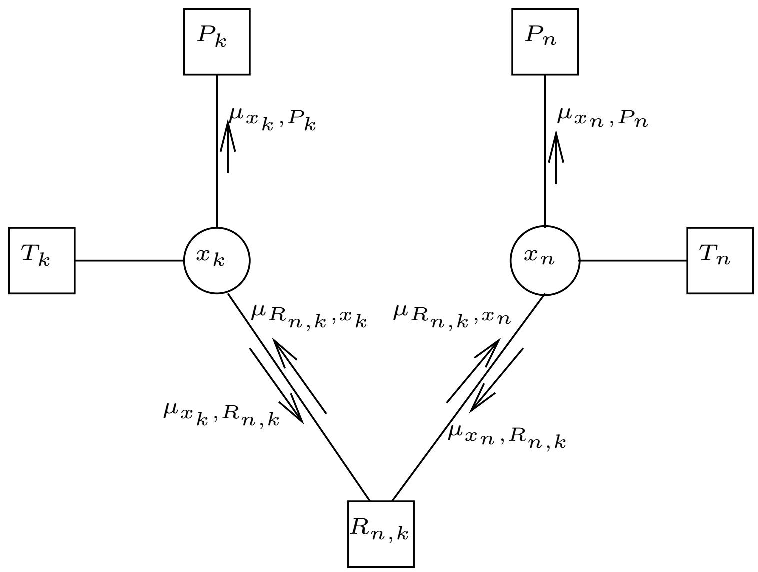

Figure 3.4: Propogated messages on the Factor Graph

By using the Fig.3.4, one can write marginalization of APPs as

$$p\left(x_n \mid \mathbf{y}\right) = Y_n\left(x_n\right) = P_n\left(x_n\right) T_n\left(x_n\right) \prod_{k \neq n} \mu_{R_{n,k} \to x_n}\left(x_n\right) \tag{3.22}$$

and the propagated messages

$$\mu_{x_n \to P_n}\left(x_n\right) = \frac{Y_n\left(x_n\right)}{P_n\left(x_n\right)} \tag{3.23}$$

$$\mu_{x_n \to R_{n,k}}\left(x_n\right) = \frac{Y_n\left(x_n\right)}{\mu_{R_{n,k} \to x_n}\left(x_n\right)} \tag{3.24}$$

$$\mu_{R_{n,k} \to x_n}\left(x_n\right) = \sum_{x_k} R_{n,k}\left(x_n, x_k\right) \mu_{x_k \to R_{n,k}}\left(x_k\right). \tag{3.25}$$

It is known from (3.5) the marginalization of a variable in a FG is product of all incoming messages. Hence Y_n is marginalization of $p\left(\mathbf{x} \mid \mathbf{y}\right)$ respect to x_n and so $p\left(x_n \mid \mathbf{y}\right)$. It is seen in (3.22) that the first two term are constant factor and the product term is updating term which means that $\mu_{R_{n,k} \to x_n}\left(x_n\right)$ bears APP information of node k about node n. It can be inferred from (3.23) that $\mu_{x_n \to P_n}\left(x_n\right)$ is proportional to the pdf $p\left(\mathbf{y} \mid x_n\right)$ and it is produced by the algorithm as extrinsic information to use in turbo iteration process. Finally, it can be said that the node $R_{n,k}$ provides the propagation of APPs between interfering variables after averaging operation.

Two of the computation methods which provide the marginal APPs from FG are Parallel-Schedule Sum-Product algorithm (PS-SPA) and Serial-Schedule Sum-Product algorithm (SS-SPA) [21]. In PS-SPA, same kind of messages are propagated at the same time for all variables therefore it has feasibility for low latency applications. PS-SPA is implemented in the given order

1-) Update all Y_n terms,

2-) Update all $\mu_{x_n \to R_{n,k}}$ messages,

3-) Update all $\mu_{R_{n,k} \to x_n}$ messages,

4-) Go to step 1 in case of not satisfying the stopping criterion,

5-) Update all Y_n terms.

In SS-SPA, the message passings are executed first in forward direction from 1 to N after operation in the backward direction from N to 1 for each variable node. The forward recursion of SS-SPA for each value of n from 1 to N is executed as given below

1-) Update the $\mu_{R_{n,k} \to x_n}$ messages for $k < n$,

2-) Update the Y_n term ,

3-) Update the $\mu_{x_n \to R_{n,k}}$ messages for $k > n$.

the backward recursion of SS-SPA can be executed for every n from N to 1

1-) Update the $\mu_{R_{n,k}\rightarrow x_n}$ messages for $k > n$,

2-) Update the Y_n term,

3-) Update the $\mu_{x_n\rightarrow R_{n,k}}$ messages for $k < n$,

and the SS-SPA is implemented through forward and backward recursion as in given order

1-) Implement the forward recursion

2-) Implement the backward recursion

3-) Go to step 1 in case of not satisfying the stopping criterion.

Due to serial implementation of SS-SPAs, latency grows linearly with the value N hence it is feasible for applications where long operation time is not much of a problem.

Since the FG including cycles cannot eliminate ISI exactly and leads to overestimation of reliability of messages propagated between nodes and factors [21]. Using $\sigma^2 = N_0/2$ greater than actual one is suggested as a very basic trick to overcome this problem in [8]. The rationale of the trick is to assume there is more noise than the actual one and thereby to decrease the reliability of propagated messages. In simulations, we use PS-SPA which is operated for one iteration. For relatively low SNR, it is not required to use N_0 greater than the actual one. For SNR values which 10^{-3} packet error rate (PER) performance is achieved, N_0 value should be generally chosen slightly higher than the actulal one.

CHAPTER 4

CHANNEL ESTIMATION, TRACKING AND INTERLEAVER DESIGN IN TIME DOMAIN

4.1 Introduction

Channel estimation is an important issue in wireless communication since provision of communication reliability is usually contingent on the quality of channel state information. Channel estimation is usually made through pilot symbols between data blocks. However, in fast fading channels, using only the pilots to estimate the channel may not be a solution of the issue since the coherence time may be smaller than data block duration. There are two solutions of this problem. One of them is to make use of pilot symbol blocks more frequently in relation to the coherence time, the other one is to track the channel with some techniques such as Least-Mean-Squares (LMS), Kalman filtering, Recursive-Least- Squares (RLS) etc. It is needed to say that using more pilots decreases throughput efficiency thereby is not preferred in many cases. Therefore, the second solution is the suitable one for the problem in our case because our interest is HF communication and the waveforms are given in Military Standard 188110-C (ML-188110C). In this study, due to lower complexity and implementation feasibility, we prefer the LMS method to track the channel. By using suitable interleaver with the channel tracking idea, channel tracking capability and the overall performance are enhanced.

In this chapter, Firstly,the system model is illustrated. Secondly, the theoretical background of how the channel estimation is made through pilot symbols will be explained. Thirdly, the pilot extension idea is explained. Then, the uni-directional

LMS channel tracking and direct application to bidirectional channel tracking will be asserted. In the interleaver design part, it is discussed why a new approach for the interleaving process is required followed by proposing of a newly designed interleaver. At the end, some corresponding results will be provided.

4.2 System Model for Receiver Part

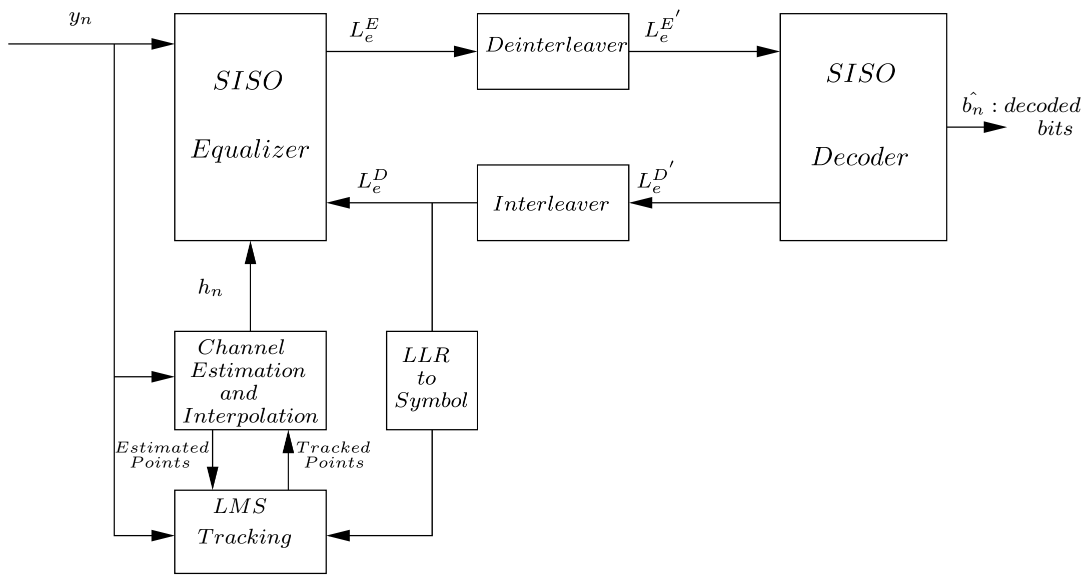

Figure 4.1: Channel estimation and tracking system model

We consider the system given in Fig. 4.1. Here, the subscript e refers to extrinsic, the superscripts E and D refer to equalizer and decoder respectively and the apostrophe represents deinterleaved case. In that case

- L_e^E: extrinsic LLR of encoded bits produced by equalizer
- $L_e^{E'}$: deinterleaved extrinsic LLR of encoded bits produced by equalizer
- L_e^D: extrinsic LLR of encoded bits produced by decoder
- $L_e^{D'}$: deinterleaved extrinsic LLR of encoded bits produced by decoder.

The receiver performs turbo equalization process which mitigates ISI iteratively. The proposed receiver performs iterative channel estimation through the following steps:

• Step 1: The channel is estimated at pilot blocks through Least Square (LS) estimation method. In order to estimate the channel coefficients in data regions, the middle points in the pilot regions are used in the interpolation process.

• Step 2: SISO equalizer performs equalization and produces L_e^E

• Step 3: Deinterleaving process is applied to L_e^E, then $L_e^{E'}$ is produced

• Step 4: The decoder performs decoding and produces $L_e^{D'}$

• Step 5: Interleaving process is applied to $L_e^{D'}$, then L_e^D is produced

• Step 6: Extended pilot sequences are produced by LLR to symbol mapping

• Step 7: The channel is tracked up to borders of extended pilot blocks by the LMS algorithm

• Step 8: Utilizing the middle points in the pilot region and the border points of the extended pilot region, a new interpolation is executed.

• Step 9: The new channel estimates are used in the equalization process.

The above process continues from step 2 iteratively.

4.3 Channel Estimation From Mini Probe

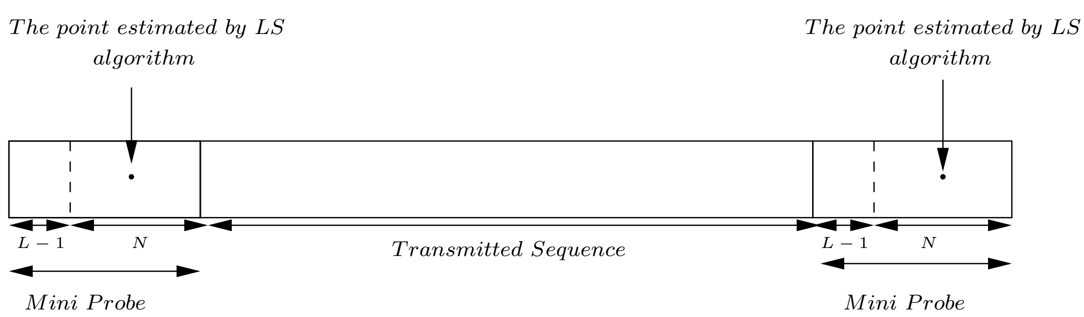

Figure 4.2: Detailed representation of pilot blocks and a transmitted sequence

The pilot blocks consist of multiple pilot symbols and referred to as mini probes in this study. Under the assumption of a time-invariant channel, channel gain coefficients can be determined by observation of mini probes at the receiver. If one wants to estimate a channel with L taps, at least L pilot symbols should be transmitted. Channel estimation becomes better as there are more than L pilot symbols in each mini probe.

Consider a transmitted signal $\mathbf{x} = [x_{-L+1}, ..., x_{N-1}]$ in a mini probe. Since the first $L-1$ observations are exposed to interference from data symbols, the received signals after these $L-1$ observation are utilized in channel estimation. The observations which are used in channel estimation

$$y_n = s_n + w_n \quad n = 0, \ldots, N-1, \tag{4.1}$$

where w_n denotes complex Gaussian noise sample and s_n is given by

$$s_n = \sum_{k=0}^{L-1} h_k x_{n-k}, \quad n = 0, \ldots, N-1. \tag{4.2}$$

Then, we can write Eq. (4.1) in matrix form as

$$\mathbf{y} = \mathbf{X}\mathbf{h} + \mathbf{w} \quad , \tag{4.3}$$

where $\mathbf{y} = [y_0, y_1, ..., y_{N-1}]^T$ and $\mathbf{h} = [h_0, h_1, ..., h_{L-1}]^T$ is channel. $\mathbf{X}$ is a $N \times L$ matrix with entries

$$[\mathbf{X}]_{i+1,j+1} = x_{i-j} \quad 0 \leqslant i \leqslant N-1, \quad 0 \leqslant j \leqslant L-1, \tag{4.4}$$

and finally $\mathbf{w} = [w_0, w_1, ..., w_{N-1}]$ is a zero mean Gaussian vector with covariance matrix

$$C_w = E\left[\mathbf{w}\mathbf{w}^H\right] = \sigma_n^2 \mathbf{I_N}. \tag{4.5}$$

We define the signal-to-noise ratio SNR of the signal as

$$SNR = \frac{\sigma_s^2}{\sigma_n^2} \tag{4.6}$$

where

$$\sigma_s^2 = \frac{1}{N}\sum_{n=0}^{N-1} \mid s\left(n\right) \mid^2 . \tag{4.7}$$

We can now write the likelihood function of $\mathbf{y}$ for given $\mathbf{h}$ as given below:

$$p\left(\mathbf{y} \mid \mathbf{h}\right) = \frac{1}{\left(\pi\sigma_n^2\right)^N} \exp\left\{-\frac{1}{\sigma_n^2}\left[\mathbf{y} - \mathbf{X}\mathbf{h}\right]^H \left[\mathbf{y} - \mathbf{X}\mathbf{h}\right]\right\} \tag{4.8}$$

We will work with the Least Square (LS) estimate of $\mathbf{h}$ which is given by [9] as

$$\widehat{\mathbf{h}} = \left(\mathbf{X}^H\mathbf{X}\right)^{-1}\mathbf{X}^H\mathbf{y}. \tag{4.9}$$

By applying this operation in all pilot regions individually, we can find the estimates at approximately middle points of all pilot blocks as shown in Fig. 4.2. Then, interpolation provides channel estimates along the whole packet.

4.4 Extension of Pilot Blocks

Finding the channel coefficients between pilots by interpolation is reasonable for slow varying channels. For instance, at $FBW = 1\ Hz$, the channel coherence time is 1 sec and the symbol duration is $1/4800 \approx 2 \times 10^{-4}$ sec in the simulations. The time

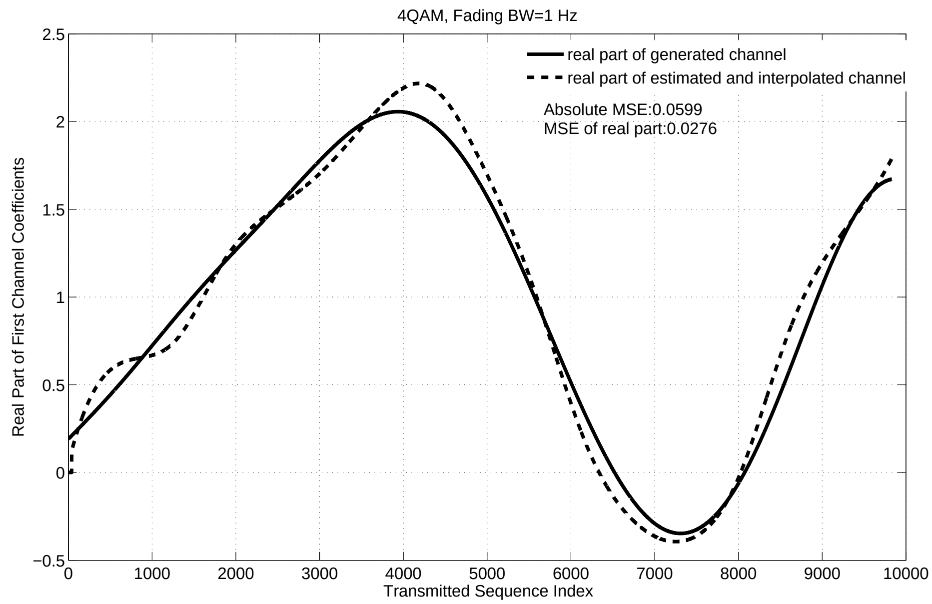

Figure 4.3: Interpolation performance along a packet under 1 Hz Doppler spread at SNR 8 dB

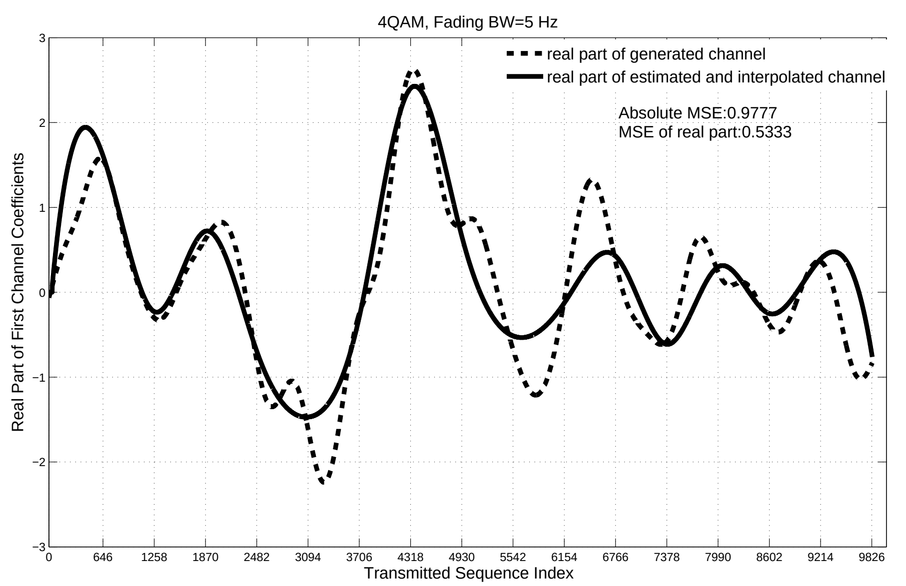

Figure 4.4: Interpolation performance of along a packet under 5 Hz Doppler spread at 8 dB

duration between pilot blocks is roughly 125 msecs. Hence , channel variation can be tracked by interpolation by pilot blocks. However, the larger the fading bandwidth is, the more the performance of interpolation diminishes. This is due to the fact that, interpolation cannot track the channel under relatively fast time variation as observed in Figures 4.3 and 4.4. Channel estimation such as in Fig. 4.4 leads to error floor as we will later observe in Section 4.5.

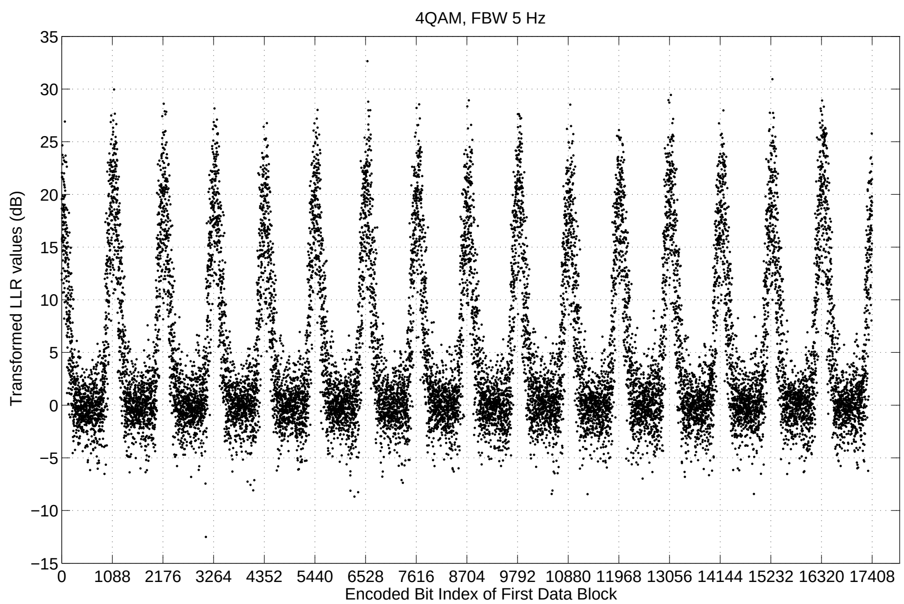

Figure 4.5: Log-likelihood-ratios of encoded bits under 5 Hz Doppler spread at SNR=8 dB for 4QAM

For FBW 5 Hz, the channel coherence time is about 0.2 sec. In such a case, we have to obtain more frequent sample points to interpolate accurately between pilot regions. This can be achieved by tracking the channel within a neighbourhood of pilot blocks. We will refer to this idea as channel estimation refinement. After the initial channel estimation, the interpolation is quite accurate around the mini probes. This leads to correct detection of those symbols after decoding. In that case, the pilot region can be extended to include a neighbourhood around the mini probes.

In Figures 4.5 and 4.6 , transformed LLR values of encoded bits after the first iteration are depicted for a typical run for 4QAM and BPSK modulation. The transformed

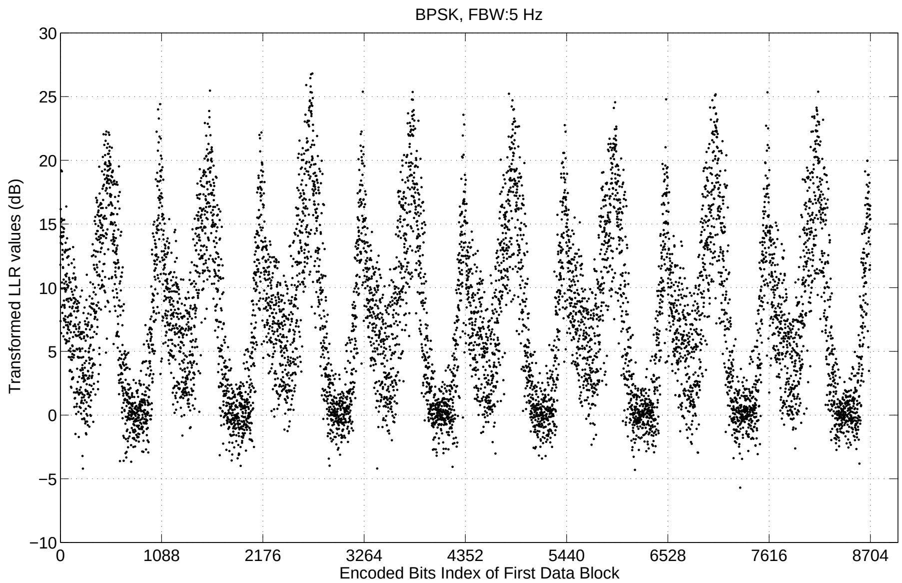

Figure 4.6: Log-likelihood-ratios of encoded bits under 5 Hz Doppler spread at SNR=8 dB for BPSK

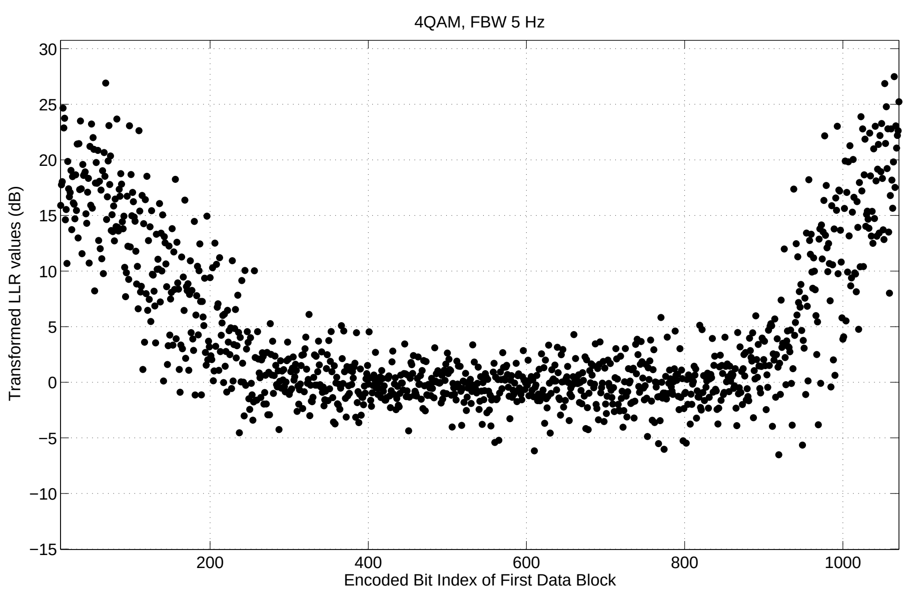

Figure 4.7: Log-likelihood-ratios of encoded bits of the first data block under 5 Hz Doppler spread at 8 dB

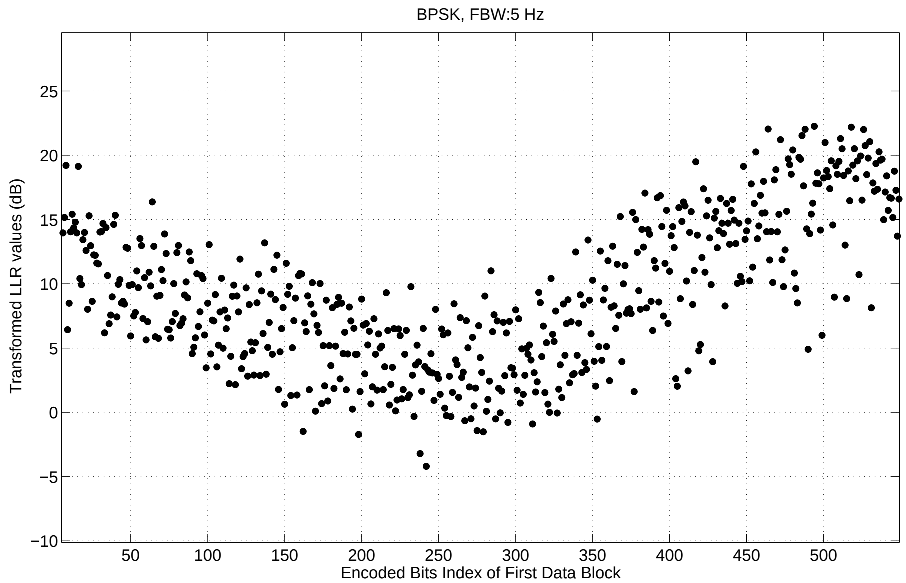

Figure 4.8: Log-likelihood-ratios of encoded bits of the first data block under 5 Hz Doppler spread at 8 dB

LLR and actual LLR are equal in magnitude but a transformed LLR is positive if the corresponding coded bit is decoded correctly. The indexed values in the figures show the data region borders. Also, it is seen that LLR values in borders neighbourhoods are greater than zero up to some certain points, which results in correct decoding of bits/symbols. In addition, it can be inferred from Figures 4.7 and 4.8 (zoomed versions of Figures 4.5 and 4.6), that the pilot blocks can be extended 50-60 symbols at 4QAM and can be extended 100-120 symbols at BPSK for both sides in the first iteration. Fig. 4.9 shows the extended pilot sequence regions. First iteration pilot region refers to extended pilot sequences after the first turbo iteration, second iteration pilot region refers to extended pilot sequences after the second turbo iteration. Furthermore, these extended pilot blocks can be used for channel tracking purposes.

It is needed to say that relatively good examples are provided in Figures 4.5- 4.8. In reality, the extension numbers are about 20-30 and 50-60 for 4QAM and BPSK respectively for such an SNR value.

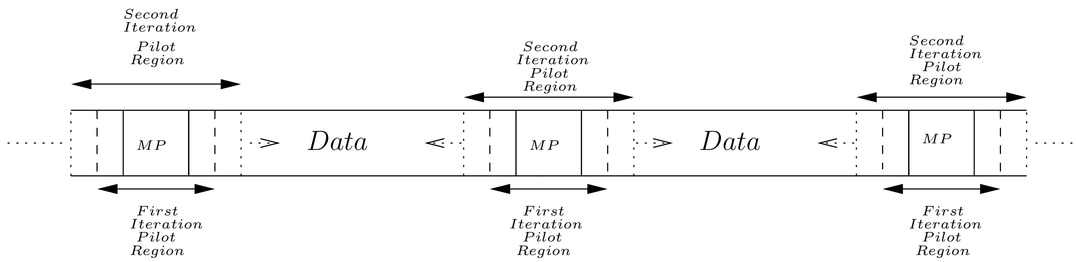

Figure 4.9: Iteratively extended pilot regions

4.5 Channel Tracking With LMS

With the LMS algorithm [19], the goal is to track the channel bidirectionally at every iteration by using the estimated channel coefficients from pilot regions. To realize the idea, firstly the channel is interpolated through the estimated points from pilots. Then, SISO equalizer generates soft information of symbols. After channel decoding operation, the training region is extended as depicted in Fig. 4.10 by means of LLR information produced by the decoder. Channel estimation is performed by LMS and interpolation enhances the channel estimation performance because of more sample points. Fig. 4.11 shows the interpolation performance with respect to iterations.

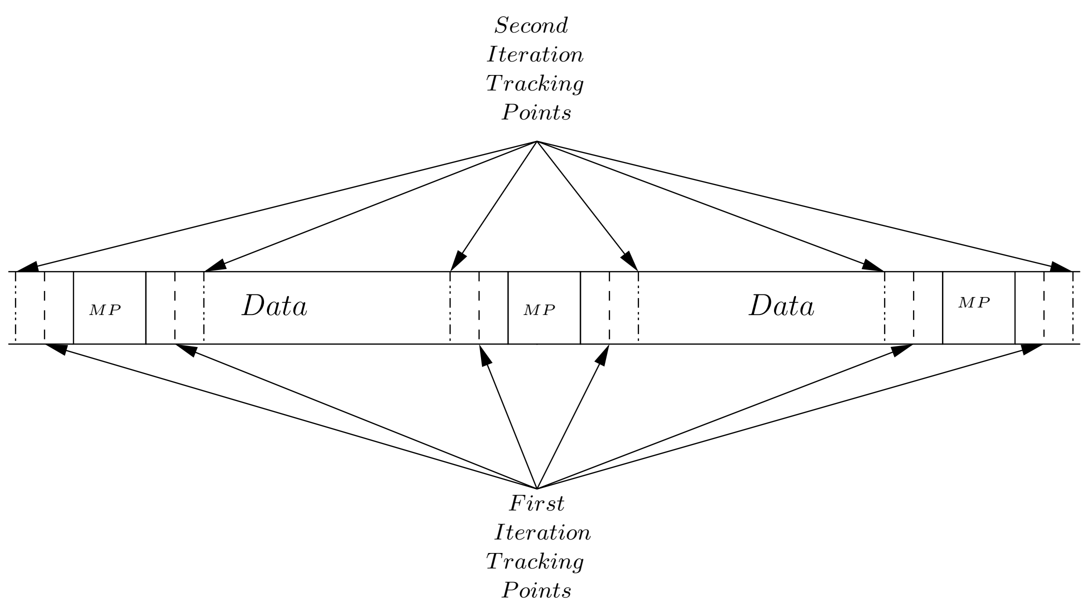

Figure 4.10: Representation of extended training points

The error signal measured at time n using the channel estimate at time $n-1$ is defined as in [24]

$$e_{n,n-1} = y_n - \hat{\mathbf{h}}_{n-1}^T \mathbf{x}_n \tag{4.10}$$

and the channel estimate at time n through the estimate at time $n-1$ is

$$\hat{\mathbf{h}}_n = \hat{\mathbf{h}}_{n-1} + \beta e_{n,n-1} \mathbf{x}_n^* \tag{4.11}$$

where $\hat{\mathbf{h}}_n = \left[\hat{h}_{n,0}, .., \hat{h}_{n,L-1}\right]^T$, $\mathbf{x}_n = [x_n, x_{n-1}, ..., x_{n-L+1}]^T$ and β is LMS tracking coefficient.

In that case, our forward and backward iterative error functions are

$$e_{n+1,n}^f = y_{n+1} - \hat{\mathbf{h}}_n^{f,T} \mathbf{x}_{n+1} \tag{4.12}$$

$$e_{n-1,n}^b = y_{n-1} - \hat{\mathbf{h}}_n^{b,T} \mathbf{x}_{n-1} \tag{4.13}$$

where f and b denote the $forward$ and $backward$ cases respectively.

Channel estimates in forward and backward directions are given as

$$\hat{\mathbf{h}}_{n+1}^f = \hat{\mathbf{h}}_n^f + \beta e_{n+1,n} \mathbf{x}_n^* \tag{4.14}$$

$$\hat{\mathbf{h}}_{n-1}^b = \hat{\mathbf{h}}_n^b + \beta e_{n-1,n} \mathbf{x}_n^*. \tag{4.15}$$

It is clear from Fig. 4.12 that the transmission performance is upgraded substantially with the iterative channel estimation refinement. At FBW 5 Hz, the equalizer cannot alleviate ISI so that error floor is observed when the channel estimation is not refined through iterative pilot extension. In contrary, the equalizer can achieve to combat ISI with by refining the channel estimation iteratively through extended pilot blocks.

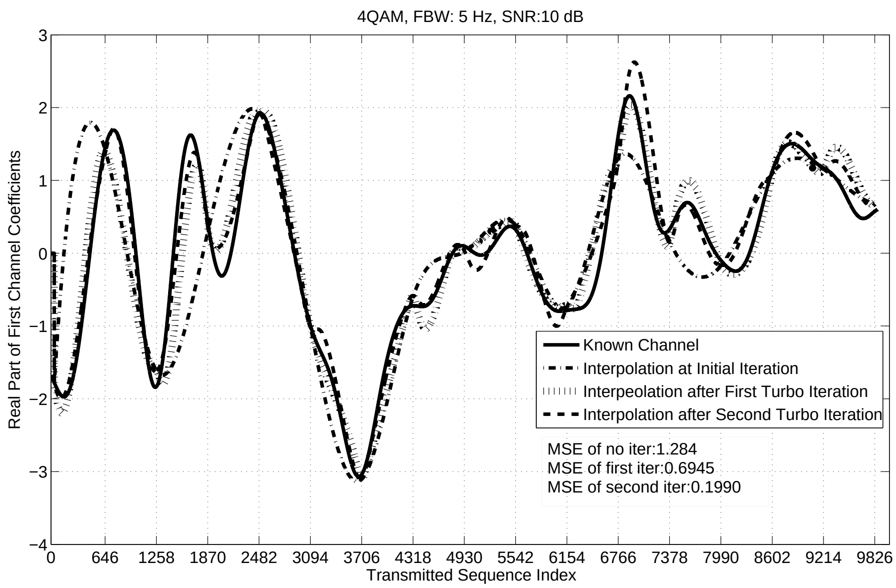

Figure 4.11: Comparison interpolated channel estimations as a function of iteration number at SNR=10 dB

For any scenario, there is a range of iterative extension number values for which the PER performance is lowest. PER curves are drawn for different scenarios in Fig. 4.13- 4.15. It can be inferred that the suitable extension number depends on modulation type. In simulations, the best ones are determined for a particular scenario after a few trials and then used throughout for the considered scenario.

Interpolation performs more accurately through well estimated points. Therefore, choosing an appropriate LMS tracking coefficient β is important to achieve a satisfactory channel tracking and interpolation performance since the channel can be tracked with small error with a proper LMS coefficient. In the study, β is determined by mean squared error (MSE) criterion through simulations for every scenario. We determine the experimentally optimum beta through 1000 randomly generated channels for every scenario where the transmitted data is known perfectly at the receiver. As observed in Fig. 4.16 and 4.17 , it is concluded that β depends on SNR and

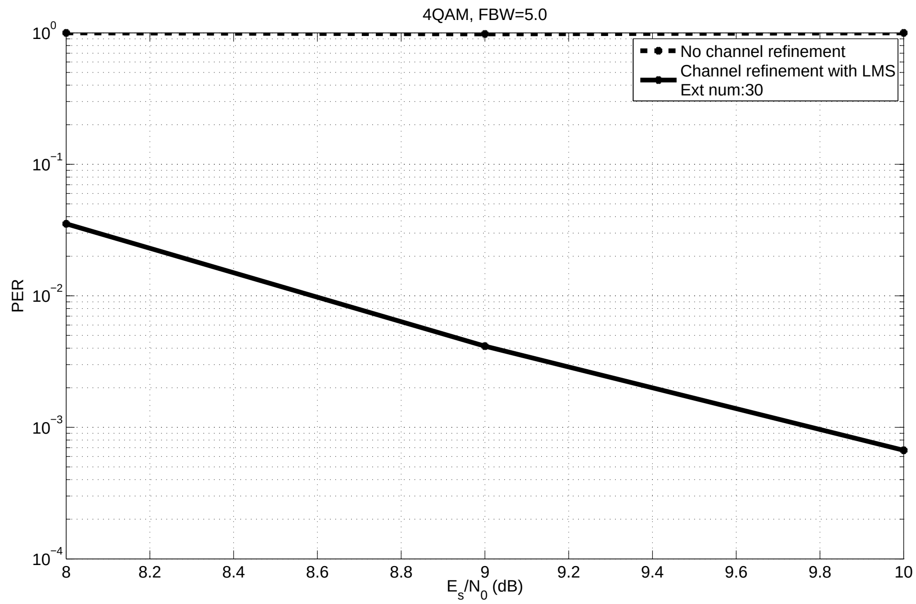

Figure 4.12: Performance comparison with and without channel estimation refinement

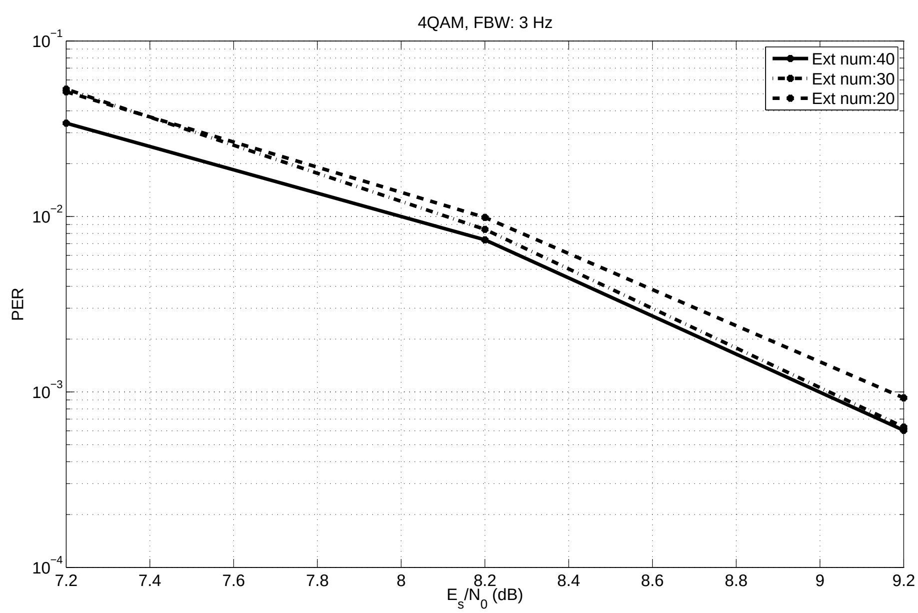

Figure 4.13: Comparison of extension numbers for 4QAM at 3Hz Doppler spread

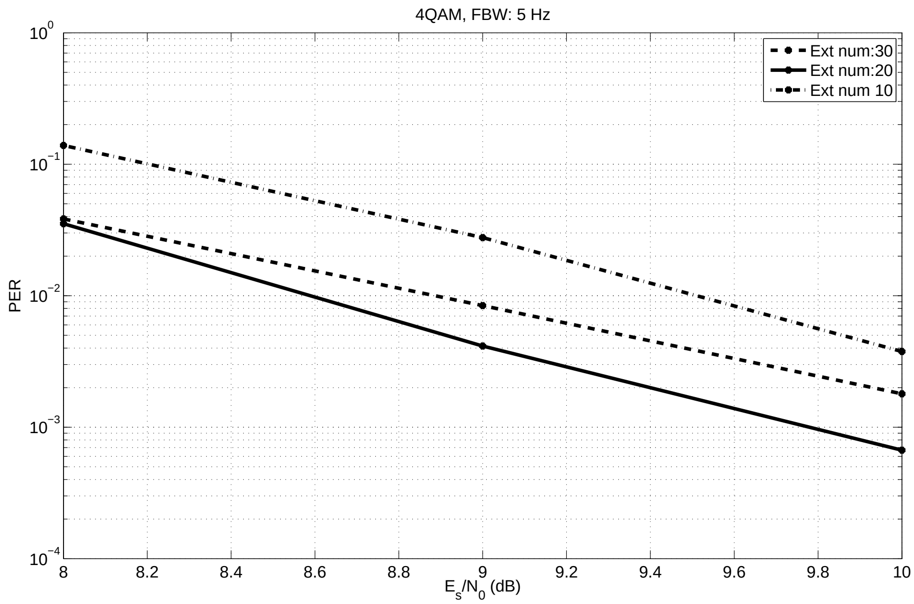

Figure 4.14: Comparison of extension numbers for 4QAM at 5Hz Doppler spread

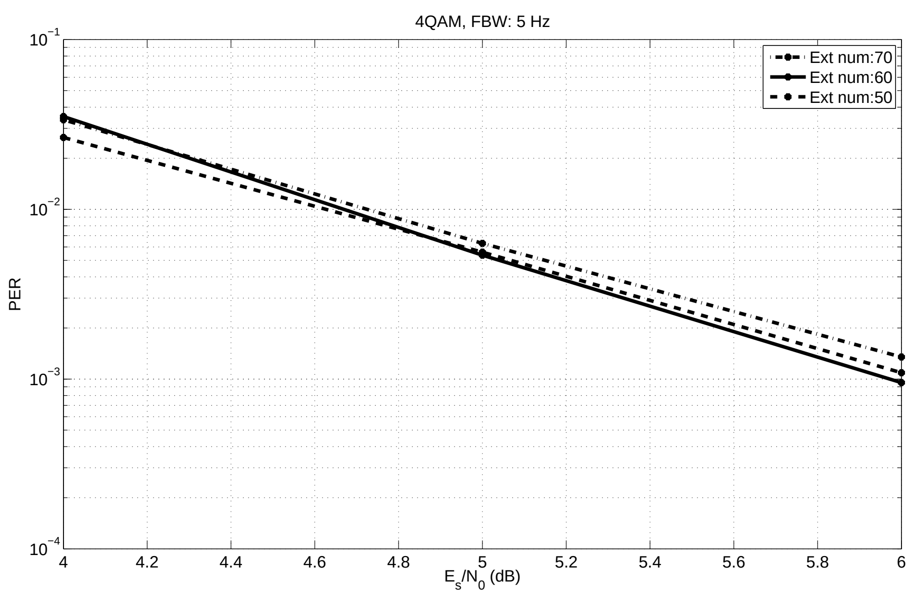

Figure 4.15: Comparison of extension numbers for BPSK at 5Hz Doppler spread

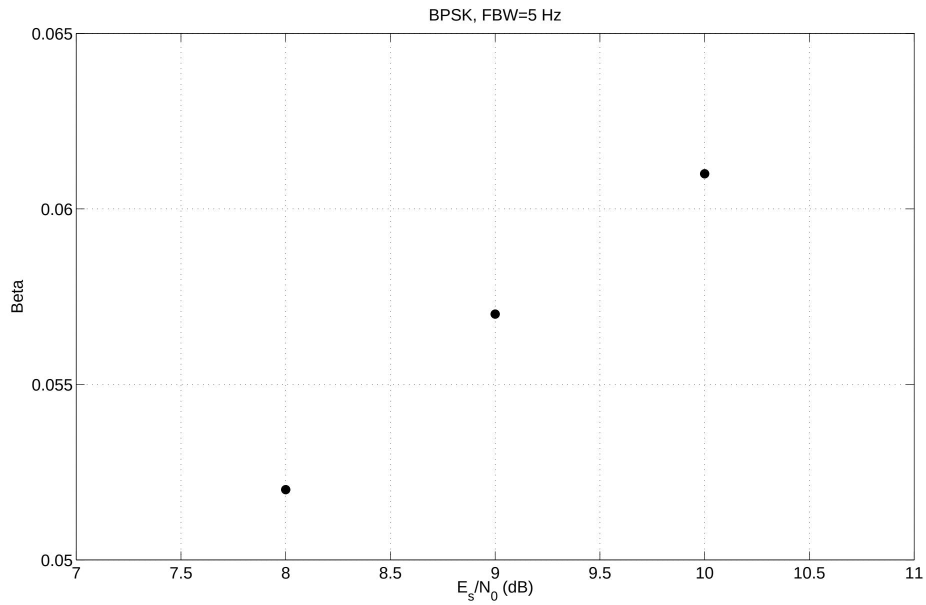

Figure 4.16: Experimentally Optimum LMS coefficients for BPSK at 5 Hz Doppler Spread

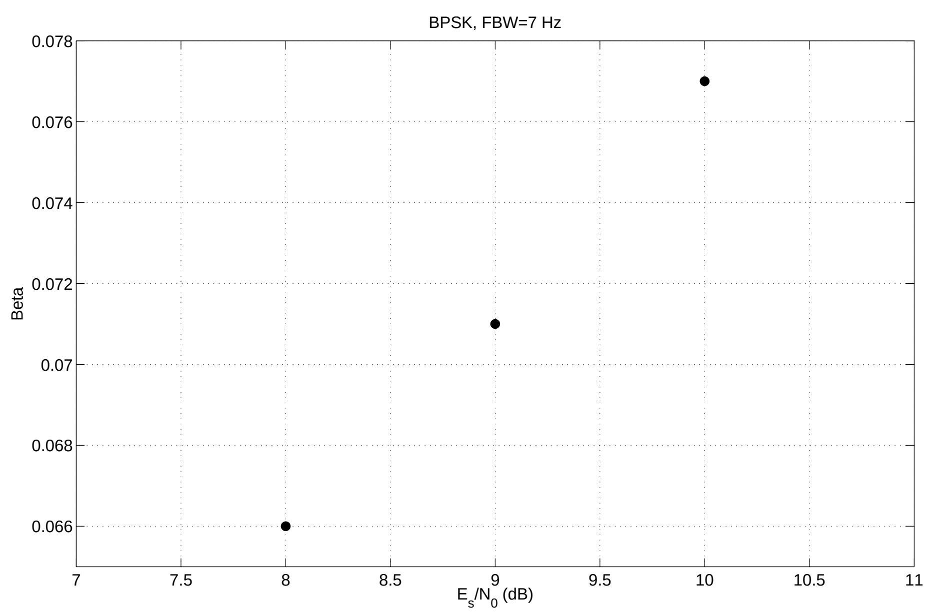

Figure 4.17: Experimentally Optimum LMS coefficients for BPSK at 7 Hz Doppler Spread

fading bandwidth.

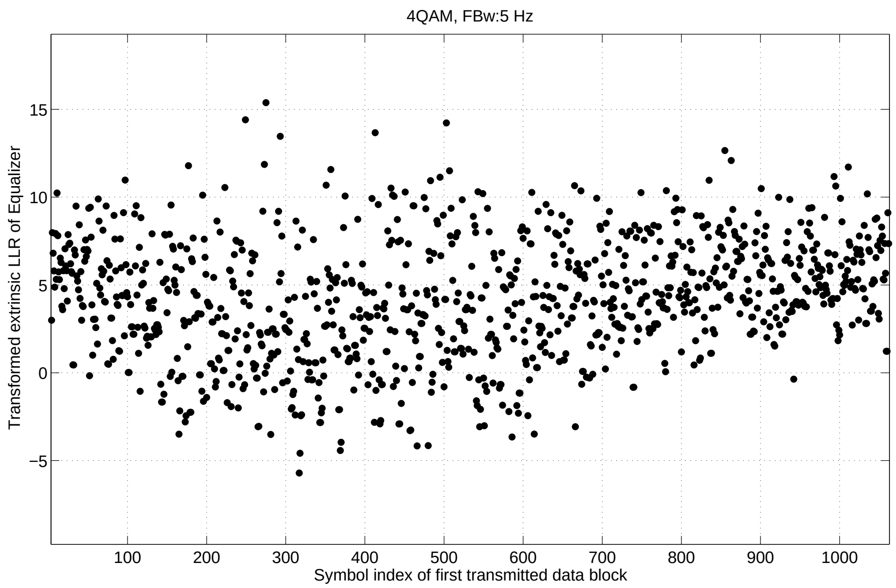

Figure 4.18: Extrinsic LLR of a data block produced by equalizer at SNR=8 dB after initial equlization

4.6 Interleaver Design

Most of the well known codes that have been devised for increasing reliability in the transmission of information are effective when the errors caused by the channel are statistically independent [26]. Error bursts are encountered in many communication media. Signals sent through channels characterized by multipath and fading phenomena are prone to fall below noise level instantaneously. If the fading duration is long enough, it leads to burst error. With interleaving, consecutive coded bits are separated out so that the channel is transformed to have almost statistically independent error characteristic. That's why, interleaving is often used as a solution to the burst error problem [26].

The interleaver used in military standard 188-110C (ML-188110C) is a block interleaver and the main aim is to separate out successive coded bits as far as possible since the HF channel is time varying fading medium. However, in relatively fast varying

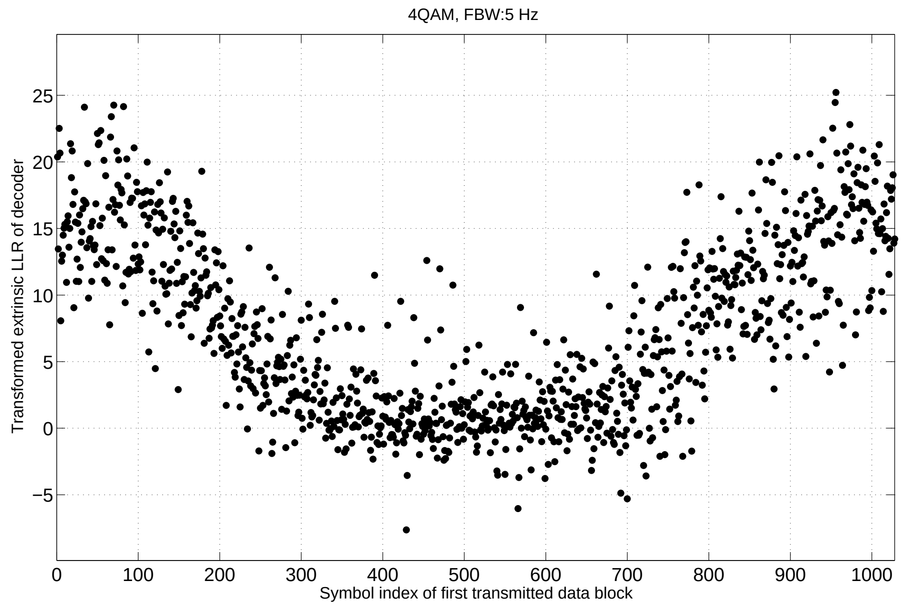

Figure 4.19: Extrinsic LLR of a data block produced by decoder at SNR=8 dB after initial equalization

changing channels, the interpolation carried out at initial iteration cannot track the channel efficiently towards the middle of transmitted data Fig. 4.4. Thereby, it is seen from Fig. 4.18 that the extrinsic LLR of equalizer L_e^E in neighbourhood of mini probes are generally more reliable than L_e^E in the middle region.

After initial equalization, the decoder makes this already reliable information even more reliable particularly in the neighbourhood of mini probes due to better channel state information. The observation can be seen in Fig. 4.19.

The symbols around the mini probe maybe used for channel estimation purposes. This corresponds to extension of training sequence. Then, the channel interpolation performance will be better since the sampling points of interpolation is far from each other. To exploit such an idea, we divide the frame into four subregions with respect to their proximity to mini probes and also divide the coded bits into four subregions. Then, we devise an algorithm which interleaves every subregion individually so that bits in a subregion don't get mixed up. This helps enhance decoding performance at the receiver. Coded and interleaved bits are modulated and sent in their own regions as shown in Fig. 4.20.

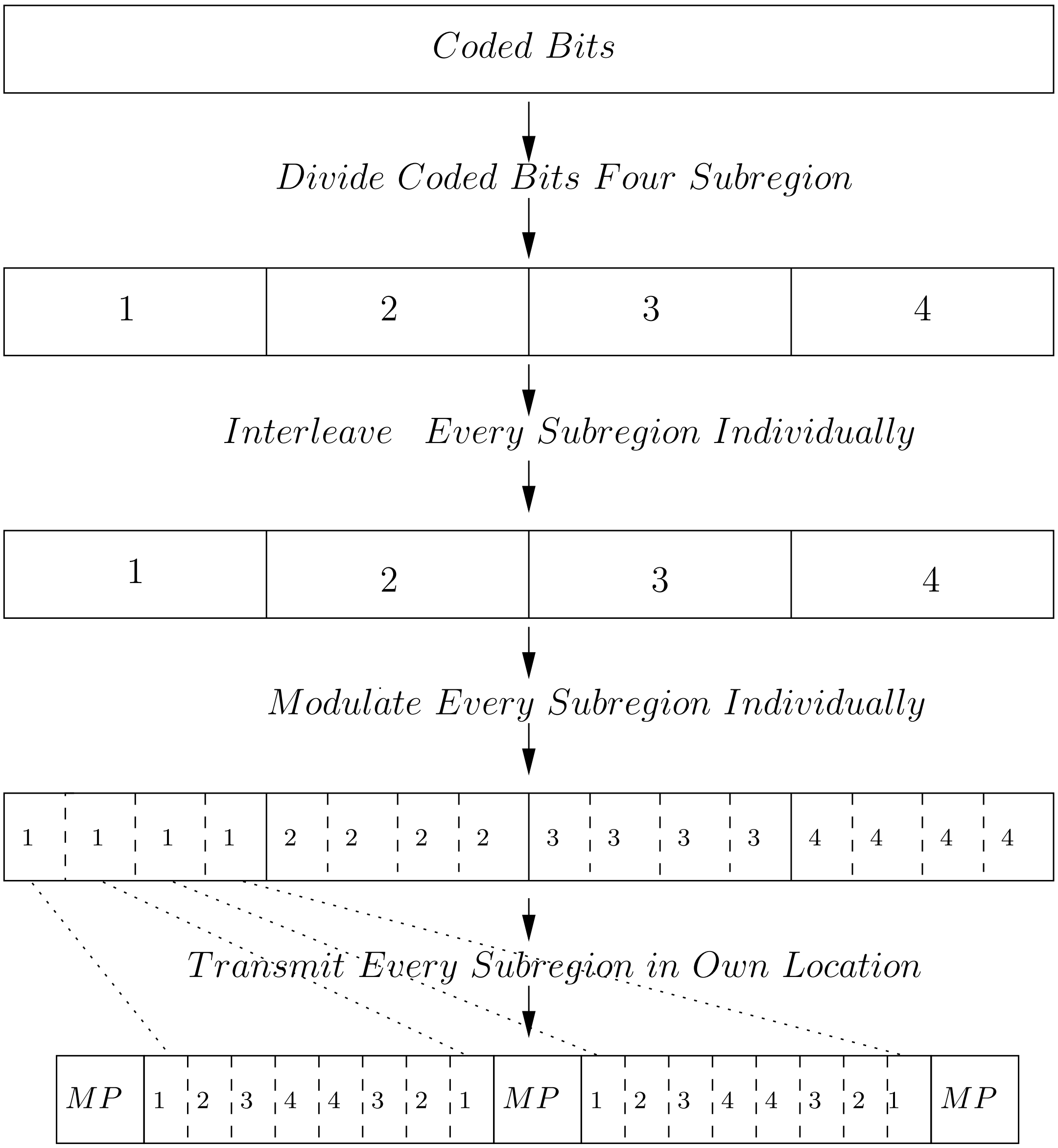

Figure 4.20: Interleaving Process

4.7 Results

We run simulations for both BPSK and 4-QAM modulations at 6 kHz baseband bandwidth and 4800 baud. The convolutional code rate is $1/2$ and constraint length is 7 with the generator polynomial $(133, 171)$. In simulations, we assume exact synchronization so that there is no frequency offset between transmitter and receiver clocks and no need for synchronization preamble. The Watterson channel model [29] is used in simulations and is equal power two tap fading channel with Gaussian power spectral density. The simulations are carried out until 50 packet errors are recorded in every case. The term "no channel refinement" indicates that the channel is estimated only from mini probes and there is no iterative estimation refinement, "known channel" indicates channel state information is perfectly known at the receiver. The term "designed intrlvr" and "ML-188110C intrlvr" point out that the channel estimation refinement is performed with the use of stated interleaver. For FBW 5 and 7 Hz, there is no "no channel refinement" result since error floor occurs. The N_0 term in used SISO equalizer is chosen 1 for any SNR value which the PER performance is lower than 10^{-3} and chosen 1.5 unless otherwise stated for the SNR values which provides 10^{-3} PER. The used iterative extension number is represented in legend.

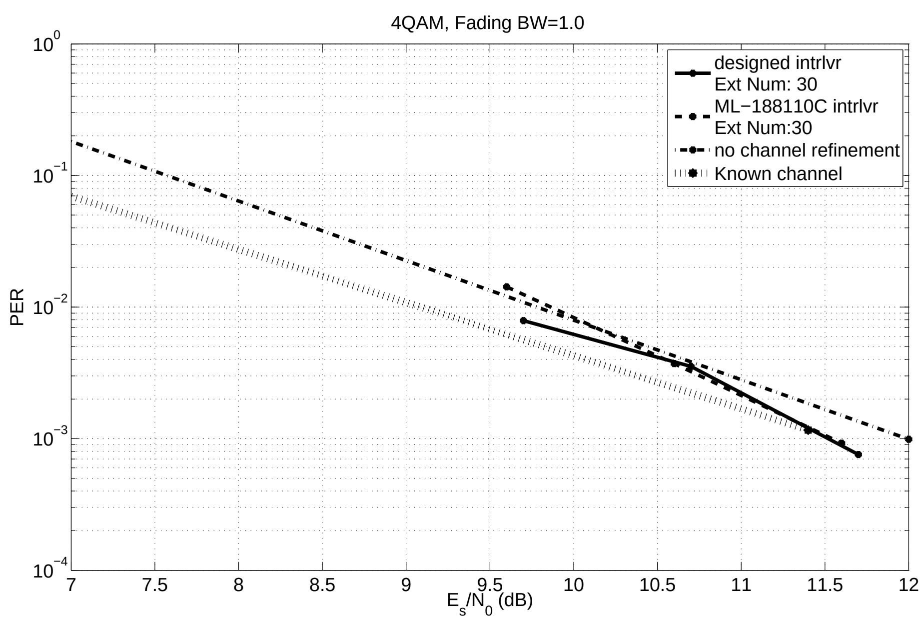

Figure 4.21: Performance comparison of various schemes for 4QAM at FBW 1 Hz

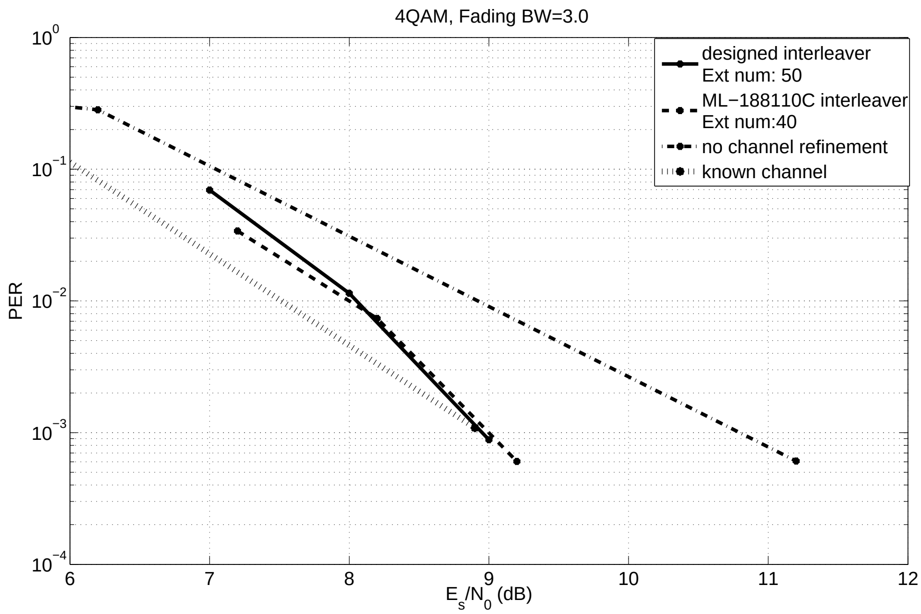

Figure 4.22: Performance comparison of various schemes for 4QAM at FBW 3 Hz

In Fig. 4.22,PER curves for FBW 3 of Hz are depicted in various cases. The performance of channel estimation refinement is the same as with "known channel" case for both interleaver types. Estimation refinement has about 2 dB SNR gain respect to "no estimation refinement" case and the SNR gain is highly satisfactory. Also, we can say that the refinement idea is useful but the designed interleaver is not required.

In Fig. 4.21, PER curves with FBW of 1 Hz are depicted for various cases. The performance of channel estimation refinement is the same as with the "known channel" case for both interleaver types. Estimation refinement provides about 0.5 dB gain with respect to "no channel refinement" case. We can say that the estimation refinement is benefical but designed interleaver has no effect on performance.

In Fig. 4.23 and 4.24, PER curves with FBW of 5 Hz are depicted for BPSK and 4QAM. The "known channel" case performance of 4QAM is better than 4QAM performance of known channel at FBW 3Hz due to diversity. It is seen that the performance of channel estimation refinement is highly satisfactory for both modulation types since the equalizer cannot eliminate ISI because of the very poor channel state information in case of there is no estimation refinement. The "no channel refinement" cannot recover any packets so that PER always 1 for all SNR values and thus not

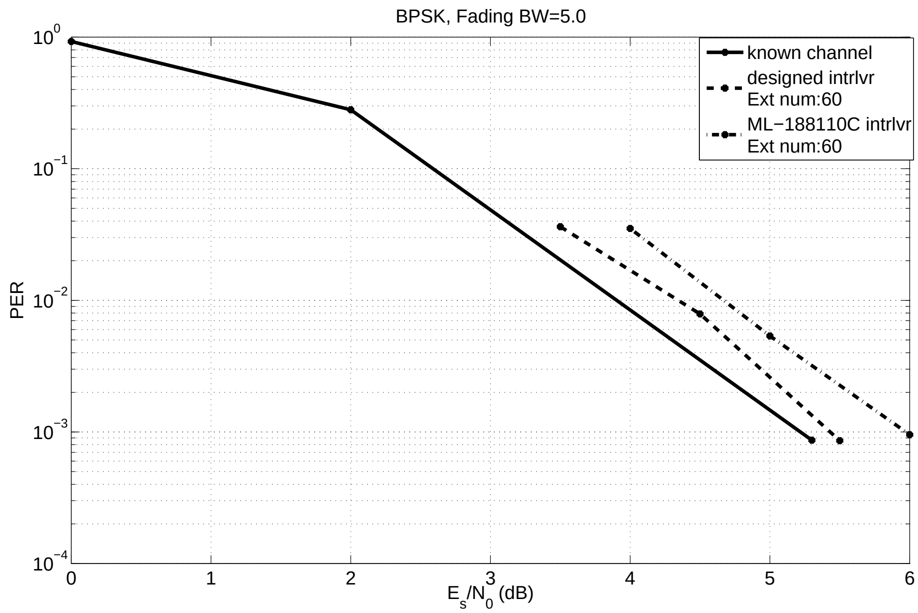

Figure 4.23: Performance comparison of various schemes for BPSK at FBW 5 Hz

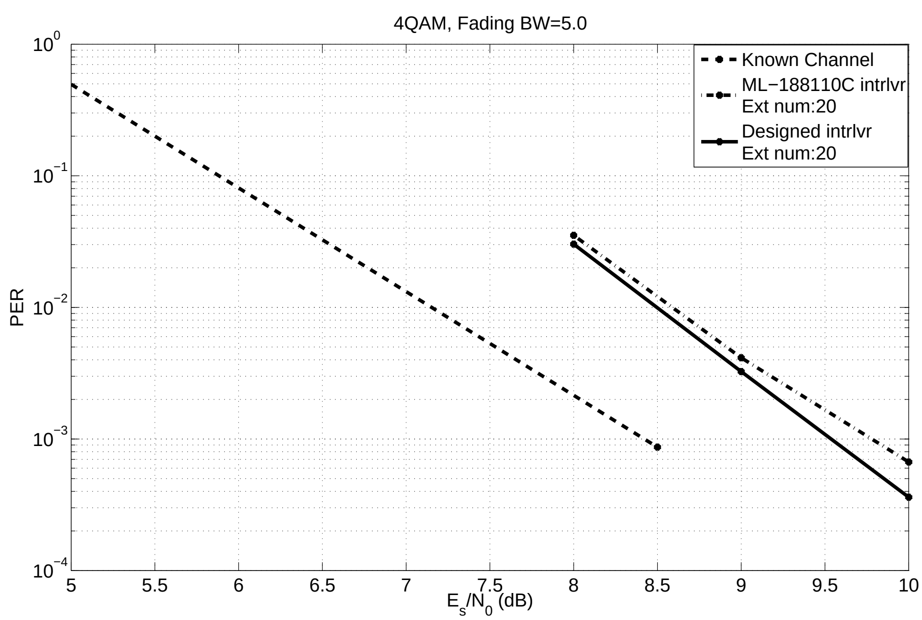

Figure 4.24: Performance comparison of various schemes for 4QAM at FBW 5 Hz

drawn in the figure. The estimation refinement performance in BPSK is almost the same as with the "known channel". The estimation refinement in 4QAM is about 1 dB off from the "known channel" case for the designed interleaver and the performance difference is reasonable. The results shows that the estimation refinement idea is pretty good for 5 Hz fading bandwidth. However, the interleaver gain difference between ML-188110C and newly designed interleaver is 0.5 dB and 0.25 dB respectively BPSK and 4QAM.

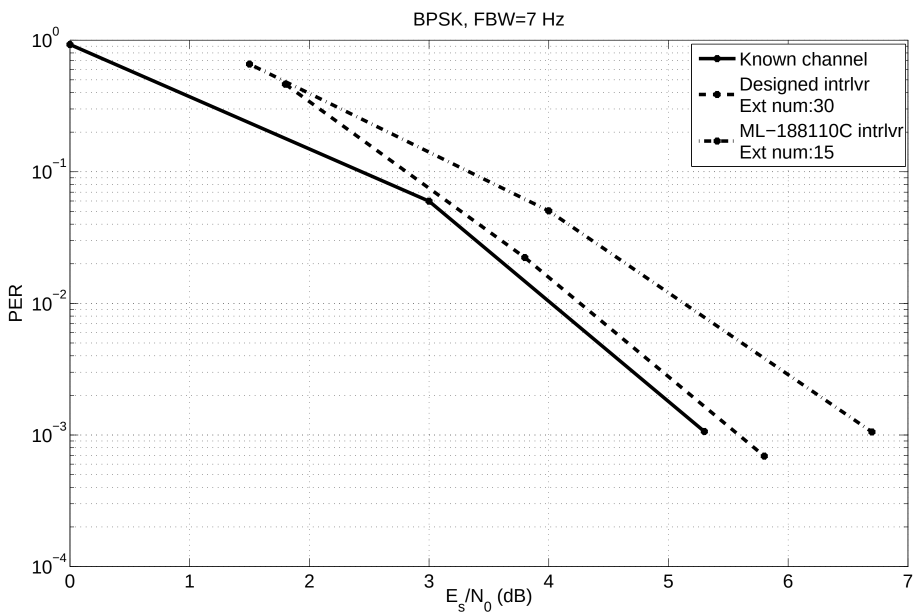

Figure 4.25: Performance comparison of various schemes for BPSK at FBW 7 Hz

In Fig. 4.25 , PER curves with FBW of 7 Hz are depicted for BPSK. The "known channel" performance and estimation refinement performance of newly designed interleaver are almost the same with each other. Therefore, the estimation refinement idea is still reasonable for BPSK. The difference between the newly designed interleaver and ML-188110C interleaver increases with respect to FBW of 5 Hz and it is about 1 dB.

In Fig. 4.26, the performance comparison of 4QAM at FBW 7 Hz is given in the PER wise. In 4QAM case, the approach still provides communication but the difference between the known channel case and the channel refinement with newly designed

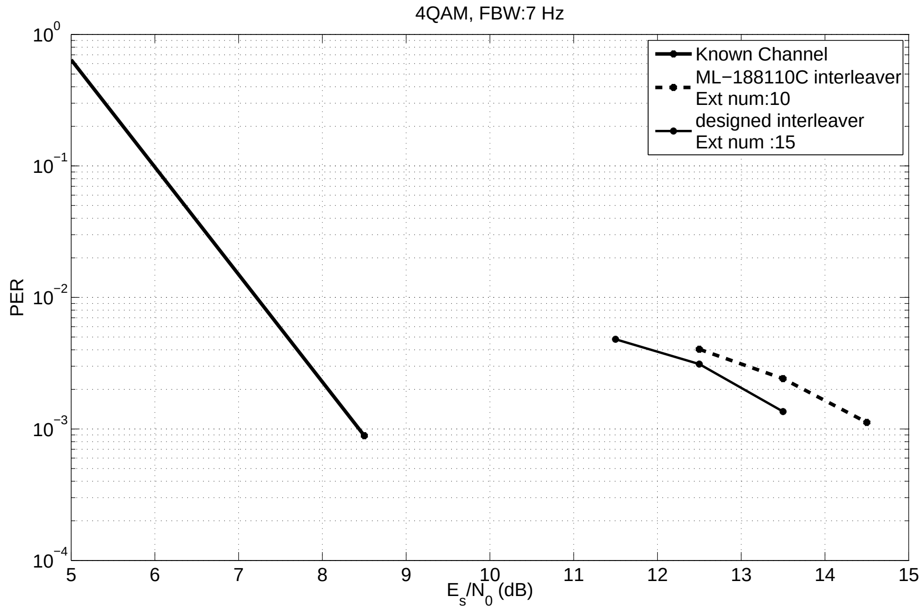

Figure 4.26: Performance comparison of various schemes for 4QAM at FBW 7 Hz

interleaver is high. We observe the limitation of the proposed scheme with these results. The result is reasonable because the coherence time of channel at FBW 7 Hz is about $150\ msec$ so that we should track the change in channel every 75 $msecs$. However, the initial interpolation is so bad that the channel cannot be extended to provide closer sample points for interpolation. Therefore, there is a huge gap between known channel and channel refinement cases.

CHAPTER 5

CONCLUSION

In wireless communication, the bearing electromagnetic waves interact with the surrounding medium which results in multipath signals. Movements of the transmitter or receiver leads to time variation in received signal power. Therefore, the wireless communication channel is characterized by ISI and fading. To provide good communication quality, channel estimation is necessary and is an integral part of the receiver since the equalizer can eliminate ISI with channel state information. Therefore, pilot sequences which are known by transmitter and receiver are utilized for channel estimation in many communication environment with some period. However, the pilot sequence is not a solution of the channel estimation problem in fast fading channels since the interpolation used with the channel estimation cannot track the channel properly. As a solution of such a problem, we propose to extend the training sequences by the aid of soft information produced by the channel decoder and to track the channel through the extended sequences to provide better interpolation. In addition, the interpolation performance at initial iteration is better at the neighbourhood of pilot sequences. Therefore, an interleaver which makes use of the better estimated region of the channel enhances the interpolation performance since it provides longer extended sequence.

As a result, the main contribution of this dissertation is given below:

- With channel tracking operated bidirectionally with LMS through the extended training sequences, interpolation capability is increased resulting equalizer performance enhancement.

• We subdivide the coded bits into subregions and interleave every subregion individually then send the transmitted symbols in their corresponding channel regions. With this application the chanel tracking capability is sometimes enhanced.

Possible future works are

• Channel tracking can be applied to OFDM transmission to estimate the channel both in time and frequency domains,

• By designing a two dimensional interleaver regarding the pilot inserting regime in the OFDM frame, the throughput as well as channel estimation and tracking performance can be enhanced.

• Performance of the proposed scheme can be investigated by using other SISO equalizers.

• Performance of the proposed scheme can be investigated by using the channel statistics in interpolation.

REFERENCES

[1] A. W. A. Oppenheim. *Signals and Systems*. Prentice Hall, 1997.

[2] G. E. B. Arslan Hüseyin. Channel estimation in narrowband wireless communication systems. *Wirel. Commun. Mob. Comput.*, pages 201–219, 2001.

[3] M. Austin, A. Buckley, C. Coursey, P. Hartman, R. Kobylinski, M. Majmundar, K. Raith, and J. Seymour. Service and system enhancements for tdma digital cellular systems. *Personal Communications, IEEE*, 6(3):20–33, Jun 1999.

[4] G. Bauch, H. Khorram, and J. Hagenauer. Iterative equalization and decoding in mobile communications systems. pages 307–312, 1997.

[5] G. Bottomley and S. Chennakeshu. Unification of mlse receivers and extension to time-varying channels. *Communications, IEEE Transactions on*, 46(4):464–472, Apr 1998.

[6] G. Bottomley and S. Chennakeshu. Unification of mlse receivers and extension to time-varying channels. *Communications, IEEE Transactions on*, 46(4):464–472, Apr 1998.

[7] J. Cavers. An analysis of pilot symbol assisted modulation for rayleigh fading channels [mobile radio]. *Vehicular Technology, IEEE Transactions on*, 40(4):686–693, Nov 1991.

[8] G. Colavolpe, D. Fertonani, and A. Piemontese. SISO detection over linear channels with linear complexity in the number of interferers. *Selected Topics in Signal Processing, IEEE Journal of*, 5(8):1475–1485, Dec 2011.

[9] S. Crozier, D. Falconer, and S. Mahmoud. Least sum of squared errors (lsse) channel estimation. *Radar and Signal Processing, IEE Proceedings F*, 138(4):371–378, Aug 1991.

[10] P. V. David Tse. *Fundamentals of Wireless communications*. Cambridge University Press, - edition, 2005.

[11] E. de Carvalho and D. T. M. Slock. Blind and semi-blind fir multichannel estimation: (global) identifiability conditions. *Signal Processing, IEEE Transactions on*, 52(4):1053–1064, April 2004.

[12] C. Douillard, M. Jézéquel, C. Berrou, D. Electronique, A. Picart, P. Didier, and A. Glavieux. Iterative correction of intersymbol interference: Turbo-equalization. *European Transactions on Telecommunications*, pages 507–511, 1995.

[13] Giles. *On the Design of HF Radio Modems*. Ph.d. dissertation, The University of Adelaide, Australia, 1995.

[14] A. Goldsmith. *Wireless communications*. Cambridge University Press, fifth edition, 2005.

[15] D. Goodman. Second generation wireless information networks. *Vehicular Technology, IEEE Transactions on*, 40(2):366–374, May 1991.

[16] D. Goodman. Second generation wireless information networks. *Vehicular Technology, IEEE Transactions on*, 40(2):366–374, May 1991.

[17] J. M. Goodman. *HF Communications. Science and Technology*. Van Nostrand Reinhold, 1992.

[18] B. L. W. Hall, M. P. M. and Hewitt. *Propagation of Radio Waves*. The Institution of Electrical Engineers, 1996.

[19] M. H. Hayes. *Statistical Digital Signal Processing and Modeling*. J. Wiley, 1996.

[20] D. K. *Ionospheric Radio*. Peter Peregrinus Ltd., 1990.

[21] F. Kschischang, B. Frey, and H.-A. Loeliger. Factor graphs and the sum-product algorithm. *Information Theory, IEEE Transactions on*, 47(2):498–519, Feb 2001.

[22] R. W. E. Mcnicol. The fading of radio waves of medium and high frequencies. *Proceedings of the IEE - Part III: Radio and Communication Engineering*, 96(44):517–524, November 1949.

[23] R. Otnes. *Improved Receivers for Digital High Frequency Coomunications: Iterative Channel Estimation and Decoding (Adaptive Turbo Equalization)*. Ph.d. dissertation, Dept. of Telecommunications, Norwegian University of Science and Technology, Norway, 2002.

[24] R. Otnes and M. Tüchler. Iterative channel estimation for turbo equalization of time-varying frequency-selective channels. *Wireless Communications, IEEE Transactions on*, 3(6):1918–1923, Nov 2004.

[25] R. Otnes and M. Tüchler. Iterative channel estimation for turbo equalization of time-varying frequency-selective channels. *Wireless Communications, IEEE Transactions on*, 3(6):1918–1923, Nov 2004.

[26] J. Proakis and M. Salehi. *Digital communications*. McGraw-Hill Education, fifth edition, 2007.

[27] S. Song, A. Singer, and K.-M. Sung. Soft input channel estimation for turbo equalization. *Signal Processing, IEEE Transactions on*, 52(10):2885–2894, Oct 2004.

[28] J. Tugnait, L. Tong, and Z. Ding. Single-user channel estimation and equalization. *Signal Processing Magazine, IEEE*, 17(3):16–28, May 2000.

[29] C. Watterson, J. Juroshek, and W. Bensema. Experimental confirmation of an hf channel model. *Communication Technology, IEEE Transactions on*, 18(6):792–803, December 1970.

[30] J. Wu and A. Aghvami. A new adaptive equalizer with a channel estimator for mobile radio communications. In *Communications, 1995. ICC '95 Seattle, 'Gateway to Globalization', 1995 IEEE International Conference on*, volume 2, pages 998–1002 vol.2, Jun 1995.

[31] R. Ziegler, M. Al-Dhahir, and J. Cioffi. Nonrecursive adaptive decision-feedback equalization from channel estimates. In *Vehicular Technology Conference, 1992, IEEE 42nd*, pages 600–603 vol.2, May 1992.